

Europe's Lost Frontiers

General Editor
Vincent Gaffney

Volume 1

Context and Methodology

edited by
Vincent Gaffney and Simon Fitch



Europe's Lost Frontiers

Volume 1

Context and Methodology

edited by

Vincent Gaffney and Simon Fitch

general editor

Vincent Gaffney



ARCHAEOPRESS PUBLISHING LTD
Summertown Pavilion
18-24 Middle Way
Summertown
Oxford OX2 7LG

www.archaeopress.com

ISBN 978-1-80327-268-9
ISBN 978-1-80327-269-6 (e-Pdf)

© Archaeopress and the individual authors 2022

Cover: Eleanor Ramsey

This book is available in print and as a free download from www.archaeopress.com



This work is licensed under a Creative Commons
Attribution-NonCommercial-NoDerivatives 4.0 International Licence



Landing by Ava Grauls (Duncan of Jordanstone College of Art & Design).
Oil and watercolour on Japanese shōji (障子) paper. 413 x 244cm

Landing is about location, ownership, shifting land and shifting borders. The painting was conceived after talking to academics about the space between Britain and Europe, and asking the question: 'How do you paint a forgotten landscape?' Landing was made to travel and interact with different environments and can be folded up and packed away into four boxes.

Ava Grauls 11/08/2021

Dedicated to our Families
For putting up with Doggerland for longer than any families since the Mesolithic



November 2021

Europe's Lost Frontiers

Europe's Lost Frontiers was funded through a European Research Council Advanced Grant (project number 670518). The European Research Council's mission is to encourage the highest quality research in Europe through competitive funding and to support investigator-driven frontier research across all fields, on the basis of scientific excellence. The European Research Council complements other funding activities in Europe such as those of the national research funding agencies, and is a flagship component of Horizon Europe, the European Union's Research Framework Programme.



European Research Council

Established by the European Commission

Contents

| | |
|------------------------------------------------------------------------------------------------------------------------------------------------------------|------------|
| List of Figures | iii |
| General Editor's Preface | vii |
| The Lost Frontiers Team | viii |
| Authors' details | ix |
| Acknowledgements | xi |
| | |
| Chapter 1 Europe's Lost Frontiers: context and development..... | 1 |
| Vincent Gaffney and Simon Fitch | |
| | |
| Before Europe's Lost Frontiers | |
| | |
| Chapter 2 Beyond the site: A re-evaluation of the value of extensive commercial datasets for palaeolandscape research..... | 16 |
| Simon Fitch and Eleanor Ramsey | |
| | |
| Chapter 3 A description of palaeolandscape features in the southern North Sea | 36 |
| Simon Fitch, Vincent Gaffney, Rachel Harding, James Walker, Richard Bates, Martin Bates and Andrew Fraser | |
| | |
| Chapter 4 From extensive to intensive: Moving into the Mesolithic landscape of Doggerland..... | 55 |
| Simon Fitch | |
| | |
| Chapter 5 The archaeological context of Doggerland during the final Palaeolithic and Mesolithic..... | 63 |
| James Walker, Vincent Gaffney, Simon Fitch, Rachel Harding, Andrew Fraser, Merle Muru and Martin Tingle | |
| | |
| Europe's Lost Frontiers | |
| | |
| Chapter 6 The Southern River: methods for the investigation of submerged palaeochannel systems | 89 |
| Simon Fitch, Richard Bates and Rachel Harding | |
| | |
| Chapter 7 Establishing a lithostratigraphic and palaeoenvironmental framework for the investigation of vibracores from the southern North Sea | 100 |
| Martin Bates, Ben Gearey, Tom Hill, David Smith, John Whittaker and Erin Kavanagh | |
| | |
| Chapter 8 Sedimentary ancient DNA palaeoenvironmental reconstruction in the North Sea landscape..... | 112 |
| Robin Allaby, Rebecca Cribdon, Rosie Everett and Roselyn Ware | |
| | |
| Chapter 9 Palaeomagnetic analysis of cores from Europe's Lost Frontiers..... | 122 |
| Samuel E. Harris, Catherine M. Batt and Elizabeth Topping | |
| | |
| Chapter 10 Applying chemostratigraphic techniques to shallow bore holes: Lessons and case studies from Europe's Lost Frontiers. | 137 |
| Alexander Finlay, Richard Bates, Mohammed Bensharada and Sarah Davies | |
| | |
| Chapter 11 Introduction to geochemical studies within Europe's Lost Frontiers | 154 |
| Mohammed Bensharada, Ben Stern and Richard Telford | |

| | |
|---------------------------------------------------------------------------------------------------------------------------------------------------------------------------------------------------|-----|
| Chapter 12 Constructing sediment chronologies for Doggerland | 165 |
| Tim Kinnaird, Martin Bates, Rebecca Bateman and Aayush Srivastava | |
| Chapter 13 Building chronologies for Europe’s Lost Frontiers: Radiocarbon dating and age-depth modelling | 181 |
| Derek Hamilton and Tim Kinnaird | |
| Chapter 14 Simulating a drowned landscape: A four-dimensional approach to solving problems of behaviour and scale | 190 |
| Phil Murgatroyd, Eugene Ch’ng, Tabitha Kabora and Micheál Butler | |
| Chapter 15 Greetings from Doggerland? Future challenges for the targeted prospection of the southern North Sea palaeolandscape | 208 |
| Simon Fitch, Vince Gaffney, James Walker, Rachel Harding and Martin Tingle | |
| Supplementary Data | |
| Chapter 16 Supplementary data to ‘The archaeological context of Doggerland during the Final Palaeolithic and Mesolithic’ by Walker, Gaffney, Fitch, Harding, Fraser, Muru and Tingle | 217 |
| James Walker, Vincent Gaffney, Simon Fitch, Rachel Harding, Andrew Fraser, Merle Muru and Martin Tingle | |
| Chapter 17 Supplementary data to ‘Constructing sediment chronologies for Doggerbank, North Sea’ by Kinnaird, Bates, Bateman and Srivastava | 218 |
| Tim Kinnaird, Martin Bates, Rebecca Bateman and Aayush Srivastava | |
| Bibliography | 222 |

List of Figures

| | | |
|--------------|----------------------------------------------------------------------------------------------------------------------------------------------------------------------------------------------------------------------------------------------------------------------------------------------------------------------------------------------------------------------------------------------------------------------------------------------------------------------------|----|
| Frontispiece | Landing by Ava Grauls (Duncan of Jordanstone College of Art & Design) | |
| Figure 1.1 | Survey areas prior to Europe’s Lost Frontiers discussed in this chapter. (1) North Sea Palaeolandscape Project (2) Humber REC (3-4) West Coast Palaeolandscape Project. ASTER DEM is a product of METI and NASA. ETOPO2v2 is the property of the National Geophysical Data Centre, NOAA, US Dept of Commerce..... | 2 |
| Figure 1.2 | Area of Doggerland mapped by the North Sea Palaeolandscape Project (Gaffney <i>et al.</i> 2009: Figure 3.23). | 3 |
| Figure 1.3 | Red flag mapping from Gaffney <i>et al.</i> (2007: Figure 9.8). This image combines threat and uncertainty data based on distance to feature and depth of overlying sediment. The lack of sediment cover and direct association with identified features with archaeological potential rate as high threats with little uncertainty. Deep overlying deposits lying farther from recorded features rank as low threat areas but with significant levels of uncertainty..... | 4 |
| Figure 1.4 | Distribution of features located within the southern North Sea during the NSPP and BSSS projects..... | 6 |
| Figure 1.5 | Map used in the final ERC application showing course of two submerged river valleys to be targeted for coring by the Lost Frontiers project team, overlaid on NSPP project base map (Gaffney <i>et al.</i> 2007). | 8 |
| Figure 1.6 | Initial modification of the Europe’s Lost Frontiers coring programme following funding in 2016..... | 10 |
| Figure 1.7 | Additional modifications to Europe’s Lost Frontiers coring programme following BREXIT..... | 11 |
| Figure 1.8 | Final Europe’s Lost Frontiers coring programme..... | 13 |
| Figure 1.9 | Europe’s Lost Frontiers core study area (1), Cardigan and Liverpool Bays (3) and area of study added as part of the Brown Bank survey (2). | 14 |
| Figure 1.10 | Iterative research methodology within Europe’s Lost Frontiers. | 15 |
| Figure 2.1 | Timeslice at 0.076s through the Southern North Sea MegaSurvey 3D seismic dataset. The NSPP study area is outlined in blue and the extended study area discussed within this paper is outlined in red..... | 17 |
| Figure 2.2 | Graph of the frequency from the PGS MegaSurvey 3D seismic data..... | 18 |
| Figure 2.3 | Additional, original 3D datasets utilised for comparison with data generated through MegaSurvey processing.... | 19 |
| Figure 2.4 | Data comparison for survey Z3NAM1988A..... | 20 |
| Figure 2.5 | Frequency values within the 3D legacy seismic volumes assessed within this study..... | 21 |
| Figure 2.6 | Frequency values within the Parametric Echo Sounder dataset. | 22 |
| Figure 2.7 | Cross-checking between horizontal and vertical slices within the 3D dataset. (A) shows correlation across a wide area with multiple responses along highlighted line, whilst (B) shows the correlation across highlighted line for a single feature..... | 4 |
| Figure 2.8 | Features within sample area, digitised within SMT Kingdom..... | 25 |
| Figure 2.9 | Features identified within sample area, imported into an ArcGIS project..... | 26 |
| Figure 2.10 | Features within the ArcGIS project cleaned and simplified. | 26 |
| Figure 2.11 | A timeslice with opacity filters applied (B), whilst (A) is the resulting interpretation of features derived from image B. It is clear the combination of opacity filters on the timeslice supports fine resolution imaging of small-scale features within this river drainage. | 27 |
| Figure 2.12 | An RMS slice from the Outer Silver Pit area. The slice is generated from the volume between 0s and 0.1s. | 29 |
| Figure 2.13 | Base horizon layer imported from SMT Kingdom into GIS..... | 30 |
| Figure 2.14 | Areas used to split the horizon point dataset. | 30 |
| Figure 2.15 | Detail within Area 1, showing band divisions used to de-stripe the data. | 31 |
| Figure 2.16 | Interpolated raster of Area 1 prior to manual de-stripping..... | 31 |
| Figure 2.17 | Interpolated raster of Area 1 after manual de-stripping..... | 32 |
| Figure 2.18 | 3D vertical exaggeration of features within Area 1 using ArcScene. | 32 |
| Figure 2.19 | Interpolated raster mosaic after values for Area 1 and Area 2 had been re-evaluated..... | 33 |
| Figure 2.20 | A 3D Geobody Model, constructed from the seismic timeslices, and displayed within the seismic volume..... | 34 |
| Figure 2.21 | A channel visualised by cutting the geobody model to reveal the base of the channel model. By using such methods, it is possible to understand, more fully, the morphology and formation of such structures..... | 34 |
| Figure 3.1 | GIS Mapping of the features recorded by the Europe’s Lost Frontiers project. | 37 |
| Figure 3.2 | Seismic line from ‘Gauss 159B’ survey acquired in 1990 by the RGD and BGS over the Dogger Bank. A Holocene channel can clearly be seen to be incised into the underlying late Pleistocene deposits (Dogger Bank Formation). | 37 |
| Figure 3.3 | Areas divisions of landscape features within the study area. | 38 |
| Figure 3.4 | Cross section across the southern flank of the Dogger Bank. The Holocene features can be seen to incise into the underlying late Pleistocene deposits..... | 39 |
| Figure 3.5 | Example of the later Holocene reuse of pro-glacial channels. This is evidenced by smaller (black) channels cut within the main valley and the formation of dendritic feeders on the side of the valley. | 40 |
| Figure 3.6 | The main drainage channels of the Dogger Bank drain south into a major channel located at the foot of the bank and in the area of the Oyster Ground, eventually flowing to the west and into the Outer Silver Pit. | 41 |
| Figure 3.7 | Mottling of the seismic data within the Oyster ground can clearly be seen in this image. A number of small palaeochannels can also be seen through the mottling..... | 42 |
| Figure 3.8 | Area 1, early Holocene features of the Dogger Bank. The main watersheds are shown as dashed black lines, the features in the southwest of Area 1, including the Shotton River, would have been the longest-lived structures on the Dogger Bank..... | 43 |

| | | |
|-------------|-------------------------------------------------------------------------------------------------------------------------------------------------------------------------------------------------------------------------------------------------------------------------------------------------------------------------------------------------------------------------------------------------------------------------------------------------------------------------------------------------------------------------------------------------------------------------------------------------------|----|
| Figure 3.9 | Map of the Eastern Sector/Area 2..... | 44 |
| Figure 3.10 | The extent of wetland response is outlined within the red hashed area. The location of BRITICE core 147VC is marked in orange..... | 45 |
| Figure 3.11 | Interpretation of a seismic line crossing the base of the Dogger Bank area (near the area marked B in Figure 3.8) clearly shows a large channel running at the base of Dogger Bank (shown here as the DB5 unit between 141VC and 140VC) (Roberts <i>et al.</i> 2018: Figure 6)..... | 46 |
| Figure 3.12 | Cross section across the east of the Oyster ground. The topographic rise which forms the watershed is apparent..... | 47 |
| Figure 3.13 | Location of mapped features within Area 3. | 48 |
| Figure 3.14 | Topographic depressions southeast of the Outer Silver Pit (Area 3)..... | 49 |
| Figure 3.15 | Early Holocene landscape features in Area 4. | 50 |
| Figure 3.16 | Mapped palaeochannels in Area 2 flow towards the -40m bathymetric contour, below this line virtually no features are mapped. This supports the hypothesis that the axial area was a marine inlet during the Holocene/Mesolithic..... | 51 |
| Figure 3.17 | Major features, Late Palaeolithic c. 11,500 BP. | 52 |
| Figure 3.18 | Coastlines of early Mesolithic Doggerland c. 10,000 BP..... | 53 |
| Figure 3.19 | Coastlines of Mesolithic Doggerland c. 8500 BP..... | 53 |
| Figure 3.20 | Coastlines of the earliest Neolithic c. 7000 BP..... | 54 |
| Figure 4.1 | Location of the Arch-Area_1 study area is shown by a red box. Bathymetric data courtesy of EMODNET Bathymetry Portal, ETOPO1 topographic data courtesy of the NCEI and NOAA..... | 56 |
| Figure 4.2 | The NSPP 2007 interpretation of the channel system overlain on EMODNET bathymetry..... | 57 |
| Figure 4.3 | Multibeam Bathymetric image of the survey area generated through the Humber REC..... | 58 |
| Figure 4.4 | Humber REC 2D seismic line over main channel and tributary channel..... | 60 |
| Figure 4.5 | Humber REC 2D seismic line showing several strong reflectors in the main channel..... | 60 |
| Figure 4.6 | A timeslice from the 3D seismic data at 0.076s derived from the PGS Megamerge dataset. The red box is the position of the Humber REC 2D survey, and the position of vibracores VC39/39A and VC40 are shown as yellow circles. | 61 |
| Figure 4.7 | Comparison between the GIS channel outlines as derived from A) the Humber REC 2D survey interpretation and B) the NSPP survey GIS interpretation. Both are overlain on a depth surface derived from the Humber REC 2D dataset..... | 61 |
| Figure 5.1 | A) The Colinda ‘harpoon’, found within a chunk of ‘moorlog’ peat dredged from the Leman / Ower banks off the Norfolk coast in 1931 (after Flemming 2002); B) A bone point recovered from beach walking at Massvlakte 2 in the Netherlands (courtesy of Luc Amkreutz); C) An array of barbed bone points from Maasvlakte 1 off the Dutch coast (courtesy of the Rijksmuseum van Oudheden). Many other examples of organic artefacts from Dutch waters may be found in Peeters and Amkreutz (2020), Amkreutz and Spithoven (2019) and Louwe Kooijmans (1970)..... | 65 |
| Figure 5.2 | Temperature curve for the Final Pleistocene and Early Holocene (Late Glacial and Postglacial between 17 and 7 thousand years ago) as derived from Greenland Ice Core data, and redrawn from Price (2015). Note the climatic variability of the Final Pleistocene relative to that of the Holocene. | 66 |
| Figure 5.3 | Map showing the projected coastlines of Doggerland and the southern North Sea since the final millennia of the Last Glacial Maximum, with key dates for the transgression highlighted. | 68 |
| Figure 5.4 | The sites and findspots located on the map are a combination of the SplashCOS viewer database, and data points presented in Tables (5.1 and 5.2), with the exception of findspots from Norwegian waters beyond the extent of the map. See this volume, chapter 16 for further information..... | 71 |
| Figure 5.5 | Four snapshots of landscape evolution across the period of 10,000–7000 cal BP. The period in question spans both the 8.2 ka cold event, and the Storegga tsunami, and shows different stages of Doggerland as it transitioned into an archipelago and, eventually, a littoral fringe landscape..... | 76 |
| Figure 5.6 | Anders Fischer’s model for the predictive location of submerged Mesolithic sites has been used to great effect in the nearshore waters in and around Denmark. Image from Fischer (2007). The model shows potentially favourable site locations in different coastal landscapes: A) near an estuary mouth or inlet with access to a hinterland; B) in close proximity to islands, but with preference for landward situation; C) on headlands, with particular preference for (D) those offering access to sheltered waters; and E) at river mouths, with preference for (F) flat and even ground..... | 78 |
| Figure 5.7 | River Valleys active in the Mesolithic, identified through seismic survey and palaeobathymetry, and marked by blue arrows..... | 80 |
| Figure 5.8 | The location of Core ELF001A where evidence of Storegga tsunami run-up deposits in highly localised areas prompted reconsideration of the event’s impact..... | 86 |
| Figure 6.1 | The location of the Southern River is within the box on the main map. | 91 |
| Figure 6.2 | The location of the 2D seismic data shown in Figures 6.3 and 6.4 is indicated by the black line (top). The lower image is an example of the original 2D Boomer dataset used for targeting the cores within the Southern River. .. | 92 |
| Figure 6.3 | 2D Boomer data after bandpass filtering applied..... | 93 |
| Figure 6.4 | 2D Boomer data after amplitude and gain correction applied..... | 93 |
| Figure 6.5 | A combined Bathymetric and seismic data surface of the Southern River. The dendritic network is visible at the head of the river, whilst sinuosity increases as the river proceeds south towards the location of the Holocene coastline. | 96 |
| Figure 6.6 | A seismic cross section showing the position of the Humber REC core Arch VC51 and Europe’s Lost Frontier’s cores ELF006 and ELF001A..... | 97 |
| Figure 6.7 | The distinctive laminated sediments (SRF6) that produce a clear signal in the seismic data are visible in these images of cores ELF033 and ELF054..... | 98 |

| | | |
|--------------|----------------------------------------------------------------------------------------------------------------------------------------------------------------------------------------------------------------------------------------------------------------------------------------------------------------------------------------------------------------------------------------------------------------|-----|
| Figure 7.1 | Distribution of cores taken during Europe's Lost Frontiers | 100 |
| Figure 7.2 | Flow diagram illustrating pathways of samples in the laboratory. | 102 |
| Figure 7.3 | Cold storage facility for the Lost Frontiers Project at Lampeter (Left). Core recording (Right)..... | 103 |
| Figure 7.4 | Cores ELF 47 and ELF 51..... | 105 |
| Figure 7.5 | Basic lithological profiles drawn up in the Southern Valley..... | 106 |
| Figure 8.1 | Differential sedaDNA fragmentation (top) and deamination (bottom) damage patterns in Doggerland palaeoenvironments. Fragmentation expressed as the lambda parameter of the exponential distribution of sedaDNA fragment sizes. Deamination expressed as the probability of observing a C to T change at the terminal position (position 0) of the 5' end of DNA fragments, caused by cytosine deamination..... | 115 |
| Figure 8.2 | Coring sites used for sedaDNA analysis. A) Cores 1-20. B) Cores in range 21-60 over the Southern River area. C) Cores 20-60. D) Core sites selected for deep sequencing. Estimated 8200 BP coastline shown in black and estimated Storegga tsunami run up extent shown in white. The Storegga tsunami core (ELF001A) shown in grey. | 120 |
| Figure 9.1 | Locations of cores used in this study. | 122 |
| Figure 9.2 | Schematic representation of the detrital remanent magnetisation mechanism from left to right - how the acquisition of the geomagnetic field occurs in sediments. | 123 |
| Figure 9.3 | Location of the UK archaeomagnetic PSVC (Meriden: 52.43°N, -1.62°E), UK Lake Windemere sequence WINPSV_12k (Avery <i>et al.</i> 2017), and FENNOSTACK comprised of seven lake sediment sequences from four lakes (Snowball <i>et al.</i> 2007). | 124 |
| Figure 9.4 | Sampling of core ELF019 during the first sampling trip (© Erin Kavanagh)..... | 125 |
| Figure 9.5 | Palaeomagnetic analysis procedure followed when full analysis takes place. | 127 |
| Figure 9.6 | Comparison of the Inclination data isolated through PCA with associated errors against the WINPSV-12k (Avery <i>et al.</i> 2017) calibration curve. | 128 |
| Figure 9.7 | Left: Magnetic susceptibility values for core ELF001A averaged from three separate runs and corrected for drift of sensor. Features on the plot are noted in the text. Right: Image of the core for comparisons. | 129 |
| Figure 9.8 | Stratigraphic trends of the rock magnetic parameters for ELF001A. The plots show the variations in a) magnetic susceptibility, b) susceptibility of ARM, c) S-ratio, d) Saturation Isothermal Remanent Magnetisation (SIRM), e) ARM _x /SIRM ratio, f) percentage of bIRM acquired between 0-20mT, and g) the Coercivity of Remanence..... | 131 |
| Figure 9.9 | Left: Magnetic susceptibility values for core ELF002 averaged from three separate runs and corrected for drift sensor. Features on the plot are noted in the text. Right: Image of the core for comparisons..... | 132 |
| Figure 9.10 | Left: Magnetic susceptibility values for core ELF003 averaged from three separate runs and corrected for drift sensor. Features on the plot are noted in the text. Right: Image of the core for comparisons..... | 133 |
| Figure 9.11 | Left: Magnetic susceptibility values for core ELF019 averaged from three separate runs and corrected for drift sensor. Features on the plot are noted in the text. Right: Image of the core for comparisons..... | 134 |
| Figure 9.12 | The declination and inclination values plotted down core for ELF019 from the analysis of 21 samples..... | 135 |
| Figure 9.13 | Down core plot of magnetic proxies calculated for core ELF019. | 135 |
| Figure 10.1 | A summary of the benefits of typical analytical tools utilised in chemostratigraphic studies and their acronyms..... | 138 |
| Figure 10.2 | Location map of cores referred to in this paper. Bathymetric data is derived from the EMODnet Bathymetry portal - http://www.emodnet-bathymetry.eu . Topographic data derived from the NOAA ETOPO1 dataset, courtesy of the NCEI - https://www.ngdc.noaa.gov/mgg/global/ | 140 |
| Figure 10.3 | PCA of elemental data for core ELF19 showing the likely mineralogical and material drivers for variation in elemental compositions. a - component 1 and 2, b - component 2 and 3..... | 141 |
| Figure 10.4 | Chemostratigraphic zonation of core ELF19. Si/Rb likely reflects variations in grain size with higher values being more Sand (Quartz) rich and higher Rb being more Clay rich. Ca/Rb likely reflects variations in carbonate (Ca) compared to clay material. S/Rb likely reflects variations in organic material (S) to clay. Br/Ti is a proxy for salinity in wetlands (see text for references)..... | 142 |
| Figure 10.5 | Boxplots showing the correlation of observed mineralogy and chemistry within core ELF19. | 144 |
| Figure 10.6 | This figure demonstrates an excellent match in the chemostratigraphic zonation of core ELF19 and ecological biostratigraphic data..... | 146 |
| Figure 10.7 | Orkney core locations | 147 |
| Figure 10.8 | The elemental variations utilised to define the chemostratigraphic zonation in the study area. Sr/Br likely reflects variations in shell material (Sr - aragonite) and organic material (Br). Sr/Rb likely reflects variations in shell material (Sr - aragonite) and Clay (Rb). Si/Br likely reflects variations in sand (Si - Quartz) and organic material (Br). | 148 |
| Figure 10.9 | Chemostratigraphic correlation of chemo zones in wells A, B and C..... | 149 |
| Figure 10.10 | Chemostratigraphic correlation of chemo sub zones in wells A, B and C. | 149 |
| Figure 10.11 | Chemostratigraphic zonation of core ELF1A (from Gaffney <i>et al.</i> 2020). Sr likely reflects the amount of shell material (aragonite) Rb likely reflects the amount of clay, Si likely reflects the amount of sand (Quartz) and Zr the amount of detrital zircon in the core. | 150 |
| Figure 10.12 | Chemostratigraphic zonation of the Storegga tsunami deposit preserved in core ELF1A (from Gaffney <i>et al.</i> 2020)..... | 150 |
| Figure 10.13 | Comparison of the relative density of core ELF1A calculated from XRF data to the interpreted seismic data (from Gaffney <i>et al.</i> 2020). | 152 |
| Figure 11.1 | Locations of the three cores mentioned in the text..... | 155 |
| Figure 11.2 | Extracted ion chromatogram (EIC), for 71m/z showing n-alkanes in the sample ELF002. | 157 |
| Figure 11.3 | Extracted ion chromatogram (EIC) for 71m/z, showing n-alkanes in the sample ELF007 | 157 |

| | | |
|--------------|------------------------------------------------------------------------------------------------------------------------------------------------------------------------------------------------------------------------------------------------------------------------------------------------------------------------------------------------------------------------------------------------------------------------------------------------------------------------------------------------------------------------------------------------------------------------------------------------------------|-----|
| Figure 11.4 | Extracted ion chromatogram (EIC) for 71m/z, showing n-alkanes in the sample ELF009. | 157 |
| Figure 11.5 | Fatty acids found in sample ELF002. | 159 |
| Figure 11.6 | Fatty acids found in sample ELF007. | 159 |
| Figure 11.7 | Fatty acids found in sample ELF009. | 159 |
| Figure 11.8 | XRD pattern of sample ELF002. | 160 |
| Figure 11.9 | XRD pattern of sample ELF007. | 160 |
| Figure 11.10 | XRD pattern of sample ELF009. | 160 |
| Figure 11.11 | Comparison between the ELF002 pattern and the standard of quartz, berlinite and calcite. | 162 |
| Figure 11.12 | PXRD of ELF007 overlain with reference patterns of quartz, berlinite and halite. | 163 |
| Figure 11.13 | PXRD of ELF009 overlain with reference patterns of quartz and halite. | 163 |
| Figure 12.1 | Locations of cores mentioned in text. | 166 |
| Figure 12.2 | For successful OSL dating, both environmental and mineral characteristics are important: zeroing during transport and deposition is a function of environmental conditions and luminescence behaviour. | 167 |
| Figure 12.3 | Illustrative luminescence-depth plots for the Doggerland cores: illustrating, (A., ELF05B) stratigraphic breaks and temporal discontinuities, (B., ELF012) rapid sedimentation and short chronology, (C., ELF022) slow sedimentation and long chronology, (D., ELF051) stratigraphic breaks, stratigraphic progressions and cyclicity. | 169 |
| Figure 12.4 | Sampling strategy for ELF cores – illustrated with core ELF001A: (a) core, with sub-units identified; (b) core, with sampling positions indicated; (c) removal of sediment for OSL profiling, OSL dating and dosimetry. | 171 |
| Figure 12.5 | Illustrative luminescence-depth plots for ELF001A: on the left, IRSL and OSL net signal intensities and depletion indices; on the right, apparent dose and sensitivity distributions. | 172 |
| Figure 12.6 | D _e distributions for ELF001A, 90-150µm, shown relative to the stratigraphy of the core. Units for ELF001A as discussed in the text. | 177 |
| Figure 12.7 | Stored dose estimates for the 90-150µm and 150-250µm quartz fractions. | 178 |
| Figure 12.8 | Dosimetry of core ELF001A: semi-quantitative and absolute down-core variations in radionuclide concentrations. | 179 |
| Figure 12.9 | (left) Apparent vs stored dose estimates for discrete depths in core across a subset of sampled cores, encompassing terrestrial, littoral and marine deposits; (right) Quartz SAR OSL depositional ages shown relative to depth in core for the same subset of cores. | 180 |
| Figure 13.1 | Locations of cores mentioned in this chapter. | 183 |
| Figure 13.2 | Age-depth model for ELF001A. Each distribution represents the relative probability that an event occurred at some particular time. For each OSL measurement two distributions have been plotted, one in outline, which is the original result, and a solid one, which is based on the chronological model use. The other distributions correspond to aspects of the model. For example, 'start: Unit 5' is the estimated date that this litho-stratigraphic change occurred, based on the dating results. The large square 'brackets' along with the OxCal keywords define the overall model exactly. | 184 |
| Figure 13.3 | Age-depth model for ELF007. The model is described in Figure 13.2, with the exception that the outline of the radiocarbon dates is based on the simple calibration of those measurements, whereas the solid ones are the result of the modelling. | 186 |
| Figure 13.4 | Age-depth model for ELF034. The model is as described in Figures 13.2 and 13.3. | 187 |
| Figure 13.5 | Calibrated humin fraction and humic acid pairs for depths 180, 185, 193, 202, and 209cm in core ELF034. | 188 |
| Figure 13.6 | Detail of the bottom of the age-depth model for ELF034. In this detail the humin fraction and humic acid dates at each level have been plotted side-by-side, rather than combined as in Fig 13.4, to show the relationship of each result to the conservative model results for the bottom of the core. | 189 |
| Figure 14.1 | The simulation conceptual framework. | 196 |
| Figure 14.2 | 3D visualisation package, showing part of the Southern River valley terrain with simulated sea level. | 197 |
| Figure 14.3 | A 3D render of the output of the forest dynamic modelling package. | 198 |
| Figure 14.4 | Graphical output from the landscape modelling package showing areas with differing amounts of inundation over time. | 198 |
| Figure 14.5 | A screenshot of the quadtree-based large-scale modelling infrastructure, showing herbivore agents responding to resources in a landscape. The red squares show the dynamic partitioning of the environment resulting from the quadtree structure. | 199 |
| Figure 14.6 | The ELF Augmented Reality sandbox. | 200 |
| Figure 14.7 | The ELF Augmented Reality sandbox in use. | 200 |
| Figure 14.8 | The Model 1.1 simulation study area. | 201 |
| Figure 14.9 | Relative sea-level change over the last 21,000 years in the North Sea region from Glacial Isostatic Adjustment (GIA) model reconstructions (Bradley <i>et al.</i> 2011; Shennan, Bradley and Edwards 2018). | 203 |
| Figure 14.10 | Table of data showing headings. | 204 |
| Figure 14.11 | Graph showing one calendar year's data of water height and atmospheric pressure effect. | 204 |
| Figure 14.12 | Graph showing 14 year's water height data. | 205 |
| Figure 14.13 | Flowchart of the Europe's Lost Frontier models. | 206 |
| Figure 15.1 | Areas designated for windfarm development within UK and Belgian waters and survey lines associated with the Brown Bank and Southern River study areas (The Crown Estate ©, bathymetry derived from EMODNET. Topography derived from ETOPO) | 209 |
| Figure 15.2 | Survey on the Southern River estuary | 211 |
| Figure 15.3 | A flint hammerstone fragment, approximately 50mm wide, was retrieved during a 2019 survey of the Southern River valley (offshore north of the Norfolk coast) from (or near) a surface dated to 8827±30 cal BP SUERC-85715 (Missiaen <i>et al.</i> 2021). Scanned image courtesy of Tom Sparrow. | 213 |
| Figure 17.1 | Equivalent dose distributions for units 4, 5, 6 and 7 from ELF001A as histogram plots | 221 |

List of Tables

| | | |
|------------|----------------------------------------------------------------------------------------------------------------------------------------------------------------------------------------------------------------------------------------------------------------------------------------------------------------------------------------------------------------------------------------------------------------------------------------------------------------------------------------------------------------------------------------------------------------------------------------------------------------------------------------------------------------------------------------------------------------------------------------------------------------------------------------------------------------------------------------------------------------------------------------------------------------|-----|
| Table 1.1 | Numbers and area of features, excluding coastlines, identified through the NSPP and BSSS projects (2008-2012). After Gaffney <i>et al.</i> 2011: Table 5.1 | 7 |
| Table 2.1 | Additional, original 3D datasets used for cross comparison purposes. | 19 |
| Table 5.1 | Mesolithic sites and findspots from territorial waters, the nearshore zone (<12 nautical miles of the shoreline) of the North Sea basin. This table excludes submerged sites and findspots located from inland waters (rivers, inlets and estuaries) in Essex (UK) and the Limfjord (Denmark). For category Type: CF = Collection of Finds; SF = Single Find; (U) = Unstratified; (S) = Stratified. For category Dating: C14 = Radiocarbon Dating; T-C = Typo-chronology; Strat = Stratigraphically; SLC = Sea Level Curve. For Sources, BMAPA stands for British Marine Aggregate Producers Association. Age estimates are given in approximate years BC, and depth is given in metres. Some locales comprise multiple findspots, and grid references are approximate. Data primarily compiled using SplashCOS Viewer available at www.SplashCOS.maris2.nl | 70 |
| Table 5.2 | Palaeolithic, Mesolithic and Neolithic findspots from the offshore zone beyond territorial waters (>12 nautical miles of the shoreline) of the North Sea basin. For category Type: CF = Collection of Finds; SF = Single Find; (U) = Unstratified; (S) = Stratified. For category Dating: C14 = Radiocarbon Dating; T-C = Typo-chronology; Strat = Stratigraphically. For category Sources: RMO stands for Rijksmuseum van Oudheden. Age estimates are given in approximate years BC, and depth is given in metres. Some locales comprise multiple findspots, and grid references are approximate. Data primarily compiled (excluding the Southern River find) using SplashCOS Viewer available at www.SplashCOS.maris2.nl | 70 |
| Table 6.1 | Geological deposits within the study area..... | 90 |
| Table 6.2 | Seismic facies within the Southern River system | 99 |
| Table 7.1 | ELF 045, lithology table..... | 104 |
| Table 7.2 | Cores sampled in project. Abbreviations as follows: P1, profile 1, uncalibrated OSL; P2, profile 2, calibrated OSL; D, OSL sediment ages..... | 108 |
| Table 7.3 | Example of data from rapid assessment of cores samples..... | 109 |
| Table 7.4 | Detailed assessment of microfossils from ELF 047. | 110 |
| Table 7.5 | Cores selected for pollen and diatom investigation. | 111 |
| Table 7.6 | Cores samples for macrofossil analysis..... | 111 |
| Table 9.1 | Summary of palaeomagnetic sampling details with core locations..... | 126 |
| Table 9.2 | The stage of palaeomagnetic analysis carried out on each core to date: X denotes completion, P denotes partial analysis. Magnetic susceptibility carried out on obtained samples at the University of Bradford (1) and carried out using the handheld MS2K directly on the core sections (2)..... | 127 |
| Table 9.3 | Definitions of magnetic proxies referred to in text and used to characterise the magnetic minerals present..... | 130 |
| Table 10.1 | Elements commonly utilised for archaeological and paleoenvironmental research (summarised from Davies <i>et al.</i> 2015 and Chemostrat multiclient report NE118)..... | 139 |
| Table 10.2 | Likely elemental affinities for core ELF19. | 142 |
| Table 10.3 | Chemical definition of Chemo Zones and boundaries for core ELF19. | 143 |
| Table 10.4 | Integrated chemical and ecological results for core ELF19. | 145 |
| Table 10.5 | Chemical, sedimentological and environmental interpretation of chemo zones and integrated facies identification..... | 148 |
| Table 10.6 | Chemo facies identified in core ELF1A (see Gaffney <i>et al.</i> 2020 supplementary information for full discussion). .. | 151 |
| Table 10.7 | A summary interpretation of geochemical and seismic datasets..... | 153 |
| Table 11.1 | Core identifiers, location and depth..... | 155 |
| Table 11.2 | The percentage of organics and carbonates. | 156 |
| Table 11.3 | Characteristic (2 θ) values, and the d-spaces of standards and the obtained samples pattern. | 161 |
| Table 12.1 | Stored dose estimates for the 90-150 μ m quartz fractions from ELF001A (lab code, CERSA114). | 178 |
| Table 12.2 | Weighted combinations of OSL depositional ages for ELF001A. | 179 |
| Table 17.1 | Observations / inferences from preliminary OSL screening and subsequent calibrated OSL characterisation, example ELF001A..... | 219 |

The Lost Frontiers Team

University of Bradford

Dr Andrew Fraser
Dr Ben Stern
Dr Catherine Batt
Dr James Walker
Dr Philip Murgatroyd
Dr Rachel Harding
Dr Richard Telford
Dr Simon Fitch
Dr Tabitha Kabora
Micheál Butler
Mohammed Bensharada
Professor Vincent Gaffney
Sam Harris
Dr Helen McCrearey
Elizabeth Topping
Anne Harvey
Tim Squire-Watt

University of Aberystwyth

Professor Sarah Davies

University of Bath

Dr Matt Law

University of Birmingham

Dr David Smith
Eamonn Baldwin

Chemostrat

Dr Alexander Finlay

University College Cork

Dr Ben Gearey
Dr Kevin Kearney

Flanders Marine Institute

Dr Tine Missiaen
Dr Ruth Plets

National University of Ireland, Galway

Eoghan Daly

University of Glasgow

Dr Derek Hamilton

INFOMAR

Kevin Sheehan

Natural History Museum

Dr John Whittaker

University of Nottingham, Ningbo

Professor Eugene Ch'ng

PalaeoEnvironmental Research and Consultancy Services Ltd

Dr Tom Hill

Sligo Institute of Technology

Dr James Bonsall
Eithne Davis

University of Wales, Trinity St Davids

Dr Martin Bates
Erin Kavanagh

University of St Andrews

Professor Richard Bates
Dr Tim Kinnaird
Rebecca Bateman
Aayush Srivastava

University of Tartu

Dr Merle Muru
Dr Alar Rosentau

University of Warwick

Dr Rebecca Cribdon
Dr Roselyn Ware
Professor Robin Allaby
Dr Rosie Everett

Wolverhampton and Walsall Historic Environment Record

Eleanor Ramsey

Dr Martin Tingle
Dr Wendy Carruthers

Authors' details

Robin Allaby, School of Life Sciences, Gibbet Hill Campus, University of Warwick, Coventry CV4 7AL, United Kingdom

Rebecca Bateman, School of Earth and Environmental Sciences, University of St Andrews, Bute Building, Queen's Terrace, St Andrews KY16 9TS, United Kingdom

Martin Bates, Faculty of Humanities and Performing Arts, University of Wales Trinity Saint David, Lampeter, Ceredigion SA48 7ED, United Kingdom

Richard Bates, School of Earth and Environmental Sciences, University of St Andrews, Bute Building, Queen's Terrace, St Andrews KY16 9TS, United Kingdom

Catherine M. Batt, School of Archaeological and Forensic Sciences, University of Bradford, Richmond Road, Bradford BD7 1DP, United Kingdom

Mohammed Bensharada, School of Archaeological and Forensic Sciences, University of Bradford, Richmond Road, Bradford BD7 1DP, United Kingdom

Micheál Butler, School of Archaeological and Forensic Sciences, University of Bradford, Richmond Road, Bradford BD7 1DP, United Kingdom

Eugene Ch'ng, NVIDIA Technology Centre, University of Nottingham Ningbo China, 199 Taikang East Road, Ningbo 315100, China

Rebecca Cribdon, School of Life Sciences, Gibbet Hill Campus, University of Warwick, Coventry CV4 7AL, United Kingdom

Sarah Davies, School of Geography and Earth Sciences, Llandinam Building, Penglais Campus, Aberystwyth University, Aberystwyth SY23 3DB, United Kingdom.

Rosie Everett, School of Life Sciences, Gibbet Hill Campus, University of Warwick, Coventry CV4 7AL, United Kingdom

Alexander Finlay, Chemostrat Ltd., 1 Ravenscroft Court, Buttington Cross Enterprise Park, Welshpool, Powys SY21 8SL, United Kingdom

Simon Fitch, School of Archaeological and Forensic Sciences, University of Bradford, Richmond Road, Bradford BD7 1DP, United Kingdom

Andrew Fraser, School of Archaeological and Forensic Sciences, University of Bradford, Richmond Road, Bradford BD7 1DP, United Kingdom

Vincent Gaffney, School of Archaeological and Forensic Sciences, University of Bradford, Richmond Road, Bradford BD7 1DP, United Kingdom

Ben Gearey, Department of Archaeology, Connolly Building, Dyke Parade, University College, Cork, Cork City T12 CY82, Ireland

Derek Hamilton, Scottish Universities Environmental Research Centre, Rankine Avenue, Scottish Enterprise Technology Park, East Kilbride G75 0QF, United Kingdom

Rachel Harding, School of Archaeological and Forensic Sciences, University of Bradford, Richmond Road, Bradford BD7 1DP, United Kingdom

Samuel E. Harris, School of Archaeological and Forensic Sciences, University of Bradford, Richmond Road, Bradford BD7 1DP, United Kingdom

Tom Hill, PalaeoEnvironmental Research and Consultancy Service, 67 Eastfield Road, Princes Risborough, Buckinghamshire HP27 0HZ / Department of Earth Sciences, The Natural History Museum, Cromwell Road, London SW7 5BD, United Kingdom.

Tabitha Kabora, Leverhulme Centre for Anthropocene Biodiversity, University of York, York YO10 5DD, United Kingdom

Erin Kavanagh, Arts Building, University of Birmingham, Edgbaston, Birmingham B15 2TT, United Kingdom

Tim Kinnaird, School of Earth and Environmental Sciences, University of St Andrews, Bute Building, Queen's Terrace, St Andrews KY16 9TS UK

Philip Murgatroyd, School of Archaeological and Forensic Sciences, University of Bradford, Richmond Road, Bradford BD7 1DP, United Kingdom

Merle Muru, Department of Geography, University of Tartu, 46 Vanemuise Str, 51003 Tartu, Estonia

Eleanor Ramsey, Wolverhampton and Walsall Historic Environment Record, Wolverhampton City Council, Civic Centre, St Peter's Square, Wolverhampton, WV1 1RP, United Kingdom.

David Smith, Classics, ancient History and Archaeology, University of Birmingham, Edgbaston, Birmingham B15 2TT, United Kingdom

Aayush Srivastava, School of Earth and Environmental Sciences, University of St Andrews, Bute Building, Queen's Terrace, St Andrew, KY16 9TS, United Kingdom.

Ben Stern, School of Archaeological and Forensic Sciences, University of Bradford, Richmond Road, Bradford BD7 1DP, United Kingdom

Richard Telford, Centre for Chemical and Biological Analysis, University of Bradford, Richmond Road, Bradford BD7 1DP, United Kingdom

Martin Tingle, 106 Brook Street, Wymeswold LE12 6TU, United Kingdom

Elizabeth Topping, School of Archaeological and Forensic Sciences, University of Bradford, Richmond Road, Bradford BD7 1DP, United Kingdom

James Walker [Archaeological Museum](#), University of Stavanger, 4036 Stavanger, P.O. box 8600, Norway

Roselyn Ware, School of Life Sciences, Gibbet Hill Campus, University of Warwick. Coventry CV4 7AL, United Kingdom

John Whittaker, Department of Earth Sciences, The Natural History Museum, Cromwell Road, London SW7 5BD, United Kingdom.

Chapter 3

A description of palaeolandscape features in the southern North Sea

Simon Fitch, Vincent Gaffney, Rachel Harding, James Walker, Richard Bates,
Martin Bates and Andrew Fraser

Introduction

The northwest European continental shelf retains, arguably, the most comprehensive record of a late Quaternary and Holocene landscape in Europe. The landscape was extensively populated by prehistoric communities and may have been a core habitat during several periods of prehistory, but was finally and rapidly inundated during the Mesolithic as a consequence of rising sea levels (Mithen 2003: 154-157; Walker *et al.* this volume). In response to the lack of a substantive archaeological context for the period of inundation, the North Sea Palaeolandscape Project (NSPP) undertook extensive mapping of the southern sector of the North Sea in 2007 (Fitch *et al.* 2005; Gaffney *et al.* 2007). This project derived mapping from seismic geophysical data rather than the bathymetric mapping used by earlier studies. As such, the results reflected the presence of buried landscape features which were not necessarily expressed within the current seabed surface (Fitch *et al.* 2005). In 2011 funding was provided by the National Oceanographic and Atmospheric Administration (NOAA) to undertake research on the Dutch sector of the North Sea, using a mega-merge dataset provided by PGS UK Ltd. Combined, these surveys covered c. 57,000km², located over some of the longest-lived areas of the Mesolithic landscape. Building on this research, the *Europe's Lost Frontiers* Project study area now includes a larger proportion of the southern North Sea, from Northern England across to Denmark in the north and the Dover Strait in the south. This represents an area of over 188,000km² (Figure 3.1).

Background

Before considering the results of mapping within the area in detail, it is useful to examine some of the background regarding the nature of the deposits associated with the landscape. Within the *Europe's Lost Frontiers* study area, the Holocene deposits under discussion are on average located between 40 and 80 milliseconds (ms) within the seismic data, with the deepest incised fluvial systems being located c. 30m below the seabed. However, it is also important to note that there are more substantial features associated with major fluvial systems and/or reused glacial tunnel valleys within the data. For

example, within Figure 3.2 a Holocene channel can clearly be seen to cut into late Pleistocene deposits (Dogger Bank Formation) to a local depth of 75ms. For the purposes of this project, analysis generally did not include features or deposits which were not directly relevant to the project goals. For example, the Outer Silver Pit Formation (Lower Pleistocene) may be up to 80m deep locally, whilst the Markham's Hole Formation achieves 150m (Cameron *et al.* 1992; Lumsden 1986). For this reason, the Lost Frontier's dataset slices are usually derived from between 40ms to 72ms. Additional slices, between 60ms and 72ms, were used specifically to visualise local features with deeper incision but were not generally applied for the purposes of broader landscape interpretation.

Validation of this approach can be demonstrated through the integration of 2D data within the 3D framework and associated core data. For example, in the north of the study area, data from the Gauss survey (e.g. Salomonsen and Jensen 1994) was cross-correlated with the 3D survey data. The palaeochannels visualised in the Salomonsen and Jensen's (1994) survey were cored, dated and determined to be of Holocene date. More recently work by the BRITICE project, working to constrain the extents of the last glaciation, has recovered cores and materials which have also provided evidence for the Holocene landscape (Roberts *et al.* 2018). Dates of 9934 +/- 188 cal BP (SUERC-72886) obtained by BRITICE core 176VC (Roberts *et al.* 2018) evidence the emergence of the landscape during the Holocene and the presence of channel activity within the area of Doggerland. The information derived from recent work is consistent with previous mapping of Holocene formations (e.g. Cameron *et al.* 1992). Consequently, there can be confidence that the derived landscape mapping reflects data relating to the Holocene.

Broad area description of the southern North Sea

Here we will provide broad descriptions for the mapped area of the southern North Sea (Figure 3.3). These supplement the published data for the English sector of the southern North Sea provided in Gaffney *et al.* 2007, and, where overlaps exist, the version here represents a revision beyond that previously published. Further

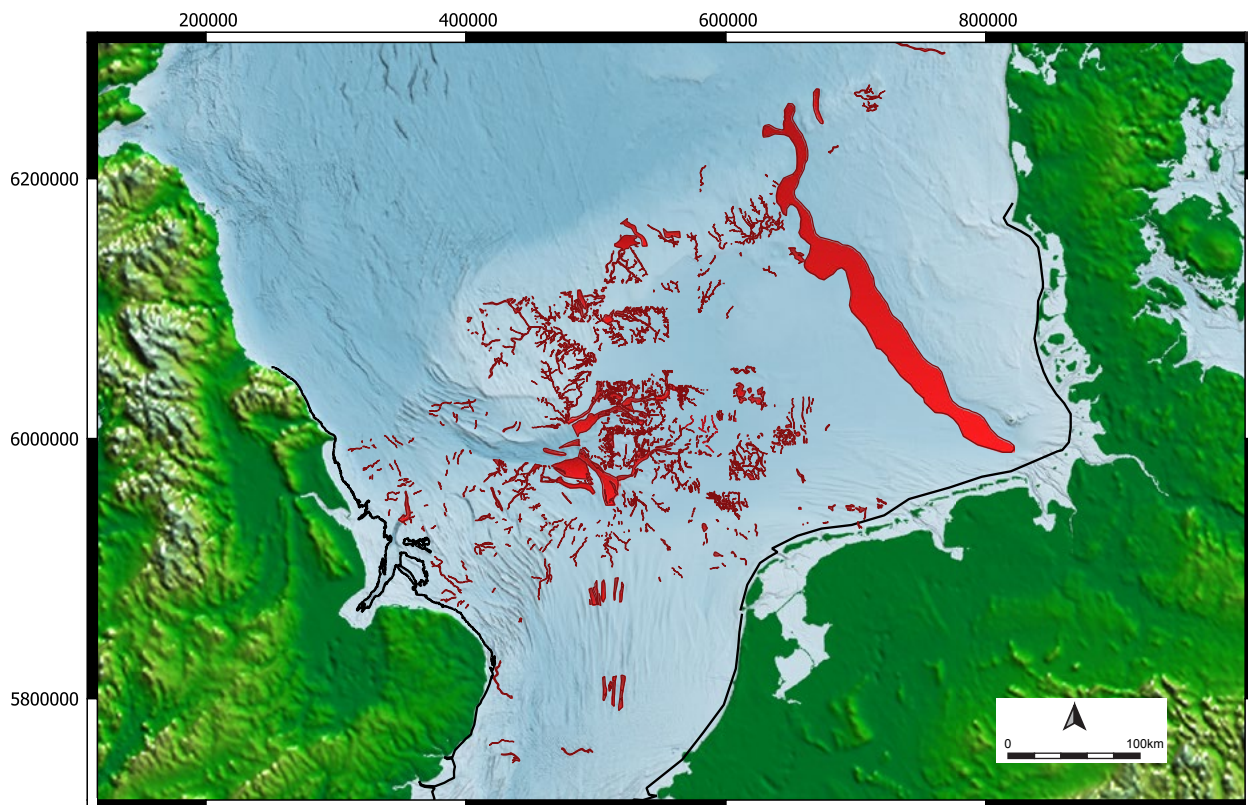


Figure 3.1 GIS Mapping of the features recorded by the Europe's Lost Frontiers project.

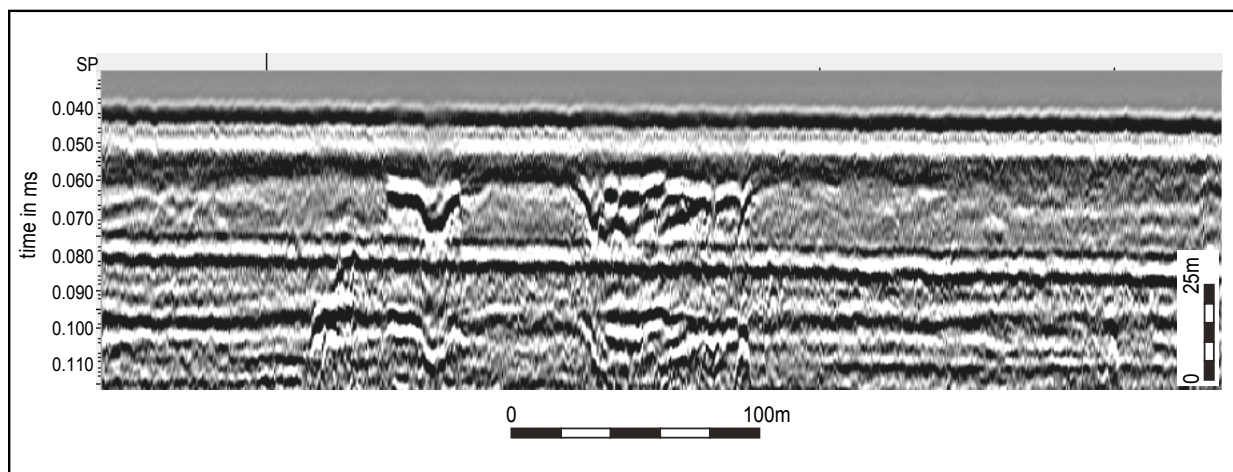


Figure 3.2 Seismic line from 'Gauss 159B' survey acquired in 1990 by the RGD and BGS over the Dogger Bank. A Holocene channel can clearly be seen to be incised into the underlying late Pleistocene deposits (Dogger Bank Formation).

detail on the areas studied by *Europe's Lost Frontiers* will be presented in later project publications.

Area 1 - Northern Sector

The landscape of the Area 1 displays the influence of the underlying late Pleistocene deposits which create an area of higher relief that gently descends into the lower lying areas surrounding the Outer Silver Pit (Figure 3.1).

On the northwest and central area of the Dogger Bank, the predominant trend of the early Holocene fluvial systems is to the south/southeast (Figure 3.8, Shotton River and A), converging on a major channel system running east/west towards the Outer Silver Pit (Figure 3.6 and Figure 3.8, B). The north/south orientation of the channels on the Dogger Bank is thought to be a relic of the late Pleistocene drainage systems of the area (Emery 2020). In the extreme north of the Dogger Bank,

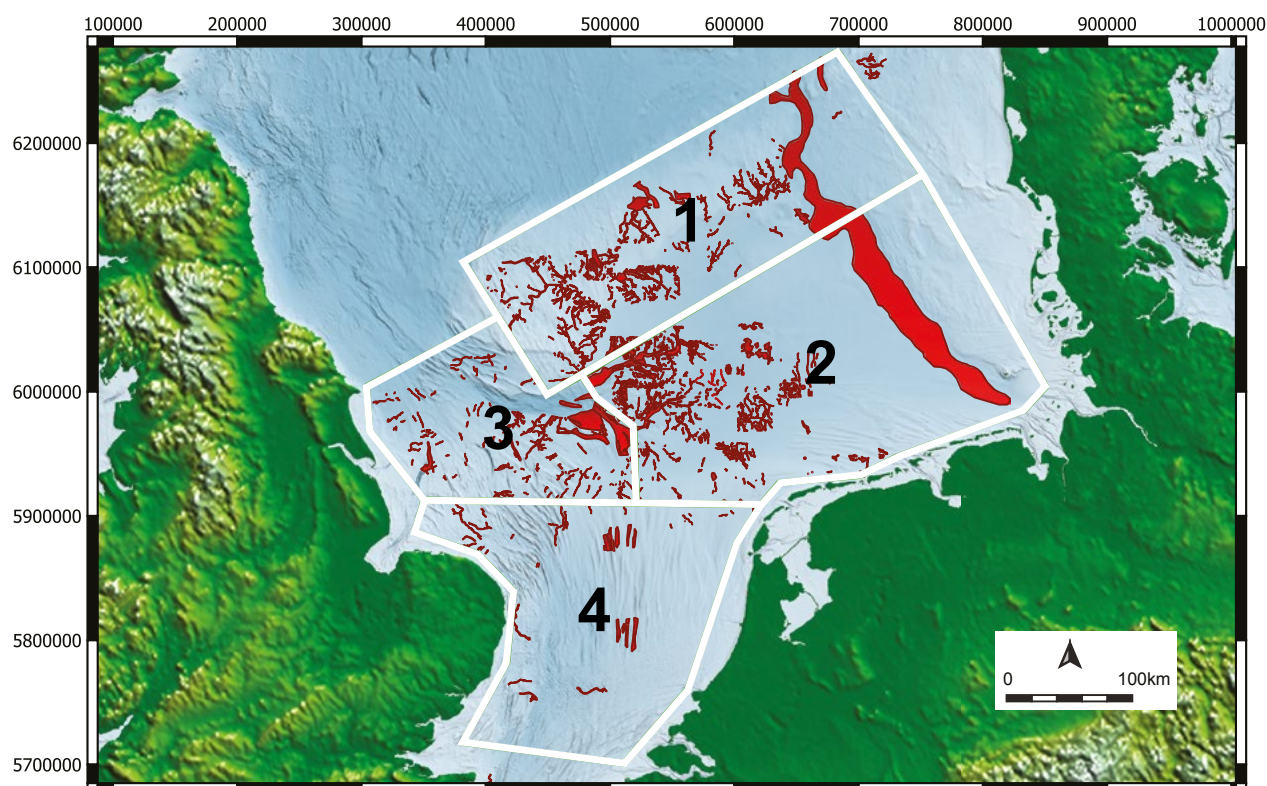


Figure 3.3 Areas divisions of landscape features within the study area.

however, one main channel runs north (Figure 3.8, C), and it is suggested that this may be a later feature with a watershed being located on the top of the Dogger Bank (Figure 3.1).

In the northeast of the Dogger Bank, the drainage directions changes. Here the channels drain from west to east into the Elbe palaeovalley. Running east of the Dogger Bank and west of Denmark, the Elbe channel was clearly a significant feature in this landscape. It has a width of 1.5km and 15m depth and can be seen clearly on seismic lines that cross the region (Hjelstuen *et al.* 2017). Smaller channels in the area were recorded by Andresen *et al.* 2019, and the wider *Europe's Lost Frontiers* data reveals these channels to be lesser tributaries of the Elbe (Figure 3.8, D). Andresen notes that these channels were formed during the Last Glacial Maximum and later morphed into sub-aerial channels. A few small channels can also be seen on the eastern side of the Elbe palaeovalley (Figure 3.18, E). These channel fragments flow to the west and towards the Elbe palaeovalley, although no data currently exists that could allow a visualisation of any junction between these channels and the Elbe itself. The exact age of these features is undetermined but, given the shallow nature of these features, they are thought to be late Pleistocene to early Holocene. As inundation progressed, these small channels would have turned into tidal channels before finally being submerged.

The Holocene fluvial features on the Dogger Bank incise the underlying late Pleistocene deposits (see Figure 3.4) and suggest that the earlier channels were active during the late Pleistocene or early Holocene, and post-date glacial activity in this area. Channel activity during this period can be divided into three main phases of activity. The first stage is seen in the formation of relatively linear channel features and is often associated with the larger features in the area. These features are of late Pleistocene age, associated with deglaciation and represent pro-glacial channels (c. 24,000 to 23,000 BP). These indicate the first stage of channel activity and end with the removal of meltwater as a source following glacial retreat. This, coupled with aridity during the period 23,000 to 17,000 BP, low temperatures and tundra conditions, caused the channels to become relict.

The second stage of channel activity in the area occurs, initially, with the reuse of earlier pro-glacial channel structures. These smaller channel systems are incised into the topographic lows associated with pre-existing structures (Figure 3.5). Aside from channel reactivation, the development of new feeders and the formation of new channel systems occurs during this period. These channels (c. 17,000 to 10,000 BP) represent an increase in channel activity due to rising precipitation after the end of glaciation (Emery 2020).

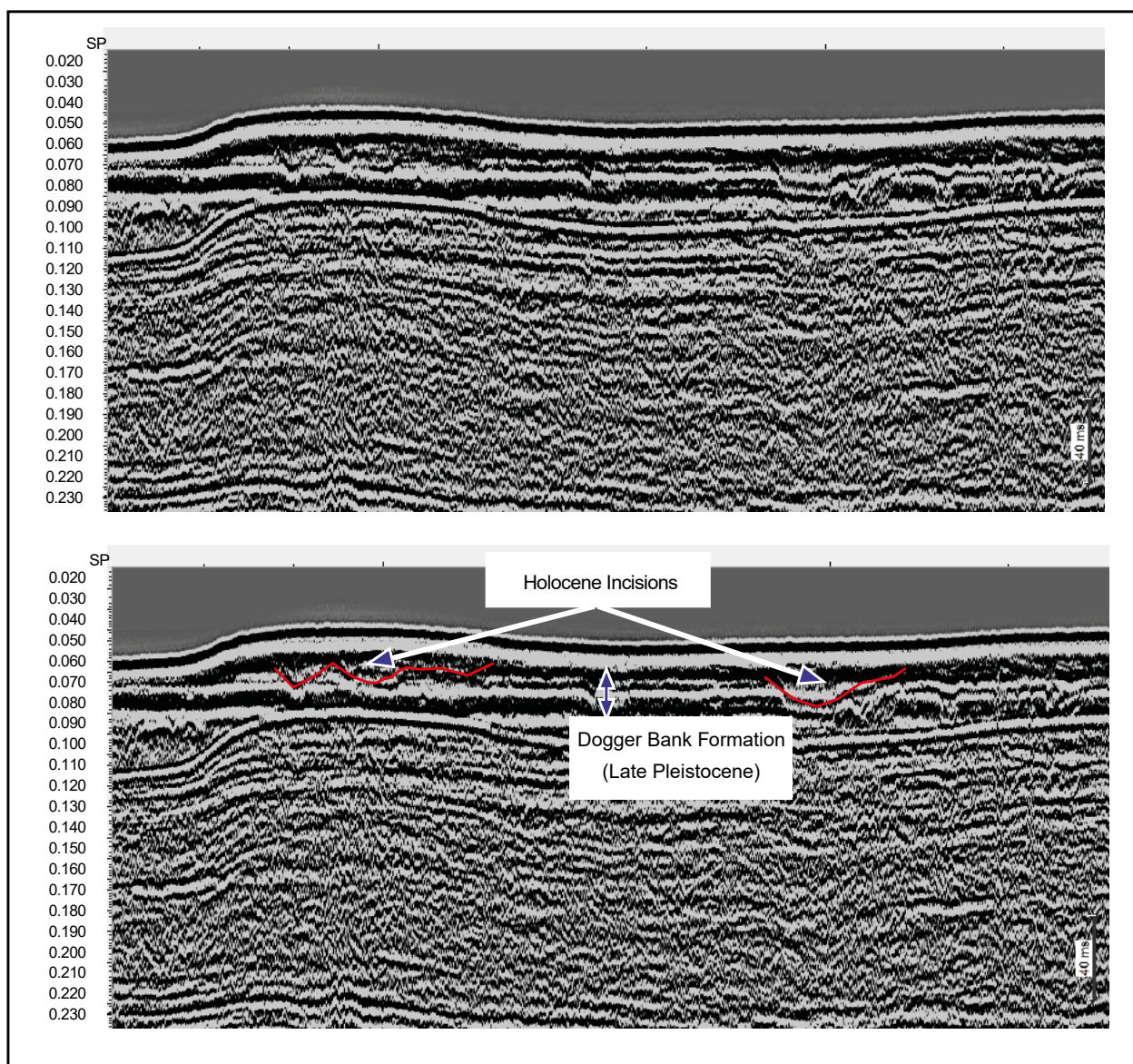


Figure 3.4 Cross section across the southern flank of the Dogger Bank. The Holocene features can be seen to incise into the underlying late Pleistocene deposits.

The geographic location of the fluvial systems on the topographic high of the Dogger Bank suggests they were sub-aerially exposed for a longer period than is evident for most of the survey area, and consequently that the systems are better developed. Roberts *et al.* 2018 suggests that the ice had retreated from this area by 23,000 BP and despite aridity during the period, a period of c. 11,000 years was available for channel development before they were inundated c. 8000 BP (Emery 2020). Most of the channels are sinuous systems with a high stream order. The channels on the Dogger Bank flow down south into a major east to west flowing channel of considerable size, located within the Oyster ground (see Figure 3.6). A vibrocore, fortuitously taken from one of the feeder tributaries of this system by the BRITICE project, provided a date of (12,629 +/- 90 cal BP SUERC-72883, Roberts *et al.* 2018: 195) which confirms the period of activity for this channel.

A third phase of channel development is evident in the area marked 'A' in Figure 3.6. Although separation of the features is difficult within the seismic data, it is clear that these later channels directly overlie the channels of the previous two stages. In addition, later channels are linked to a coastline which is related to the submergence of the landscape at around 8000 BP (Emery 2020; Shennan and Horton 2002), and therefore likely to have been formed as a response to the break-up of the landscape and a change in river base levels. Given that the channel (Figure 3.6, A) drains the top of the Dogger Bank, later channels are therefore likely to be associated with the final stages of the emergence of the Dogger Bank itself (see Figure 3.8). Zones of 'mottling' in the seismic data are associated with the flooding of the landscape and are thought to relate to peat formation (Emery 2020; Hepp *et al.* 2017). These correspond to a different seismic response in the areas



Figure 3.5 Example of the later Holocene reuse of pro-glacial channels. This is evidenced by smaller (black) channels cut within the main valley and the formation of dendritic feeders on the side of the valley.

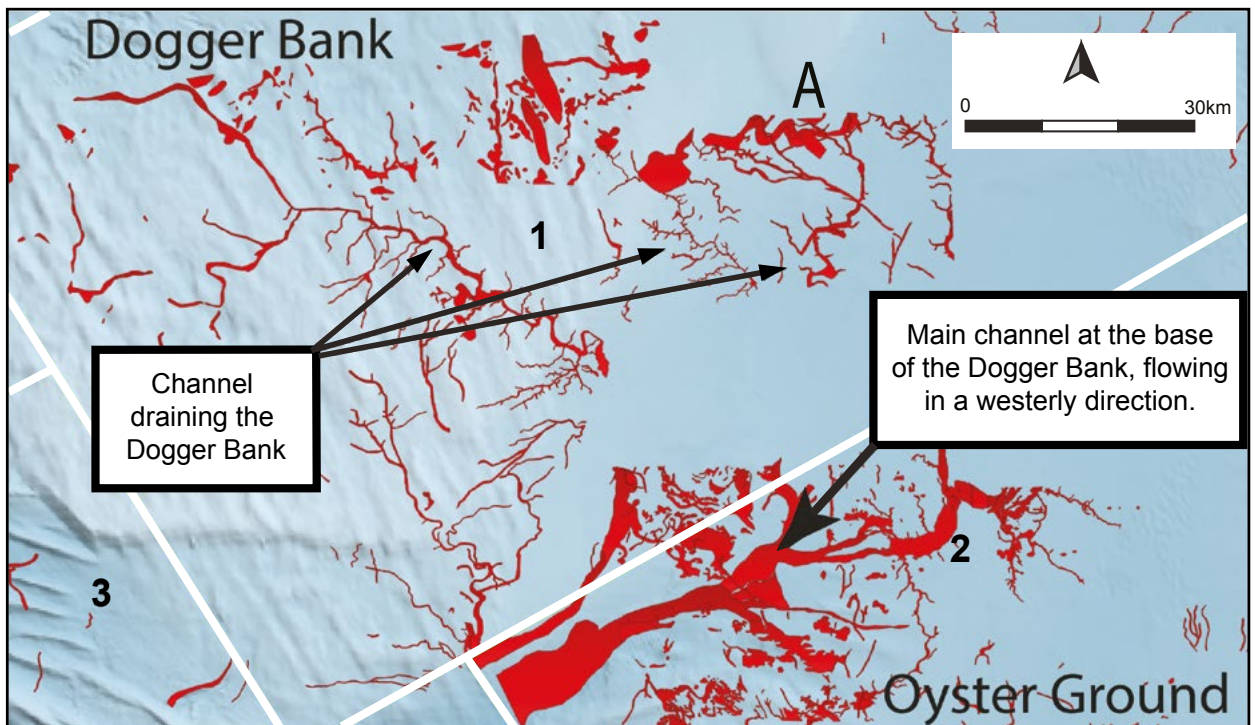


Figure 3.6 The main drainage channels of the Dogger Bank drain south into a major channel located at the foot of the bank and in the area of the Oyster Ground, eventually flowing to the west and into the Outer Silver Pit.

between the channels (Figure 3.7). This is indicative of intertidal/wetland deposits associated with inundation in this area (Hepp *et al.* 2017). The deposits are therefore likely to comprise organic muds and silts similar to deposits in the offshore Humber area (Gearey *et al.* 2017; Tappin *et al.* 2011), and thought to be of a similar Holocene age to those features dated by the Humber REC (Fitch *et al.* 2011). Within the sector, the Elbe flowed through a valley that extended across Doggerland, and is substantial enough to retain a bathymetric expression to the present day, cutting through the high ground formed by the Dogger Bank and Danish shelf. At the extreme northeast of the sector, the mouth of the Elbe palaeovalley valley can be seen clearly (Figure 3.8, F).

Seismic lines acquired across this feature show the channel relating to the Holocene to be incised some 15m below the seabed with a channel width of 3km (Hjelstuen 2017). A study by Özmaral (2017) demonstrates that the Elbe palaeovalley was almost completely devoid of pre-transgressive deposits, with the exception of sediments from a south/north trending channel network within the valley. The seismic profiles from this south/north trending channel is comparable to some of the larger channels studied by *Europe's Lost Frontiers* and suggests a similar sequence. Given the mouth of the Elbe palaeovalley is at a depth of c. 56m, which is similar to the late Pleistocene/early Holocene sea level, it is highly likely that parts of this

area of the valley were starting to be flooded at that time (Vink *et al.* 2007) and that these channel sediments relate to the brief period following deglaciation and immediately prior to submergence. Özmaral (2017) demonstrates that after inundation was initiated, the valley experienced at least three phases of sedimentary infill due to changes in sea level. This is supported by research in the Palaeo-Ems, which fed into the Elbe Palaeovalley (Hepp *et al.* 2019), which also records these three phases and suggests the onset of fully marine conditions after 9300 cal BP. This, therefore, provides a date at which the majority of the associated Elbe palaeovalley would have also been submerged.

Area 2 – Eastern Sector

There is significant striping evident in the 3D seismic data from the southeast of Area 2. Data quality is, however, reasonable elsewhere, and 2D seismic is available to supplement the 3D data. Analysis reveals the area is largely a gently sloping, emergent plain, cut by the Elbe palaeovalley. This landscape reflects the presence of deep, late Pleistocene sediments which effectively mask any topographic expression from geological movement, such as salt swells (Holford *et al.* 2007). A topographic high is evident near the modern Dutch coastline, descending towards the lower plain of the Oyster Ground, to the south of the Dogger Bank (Figure 3.9, A). However, the dominant feature in the area is the topographic low associated with the Elbe

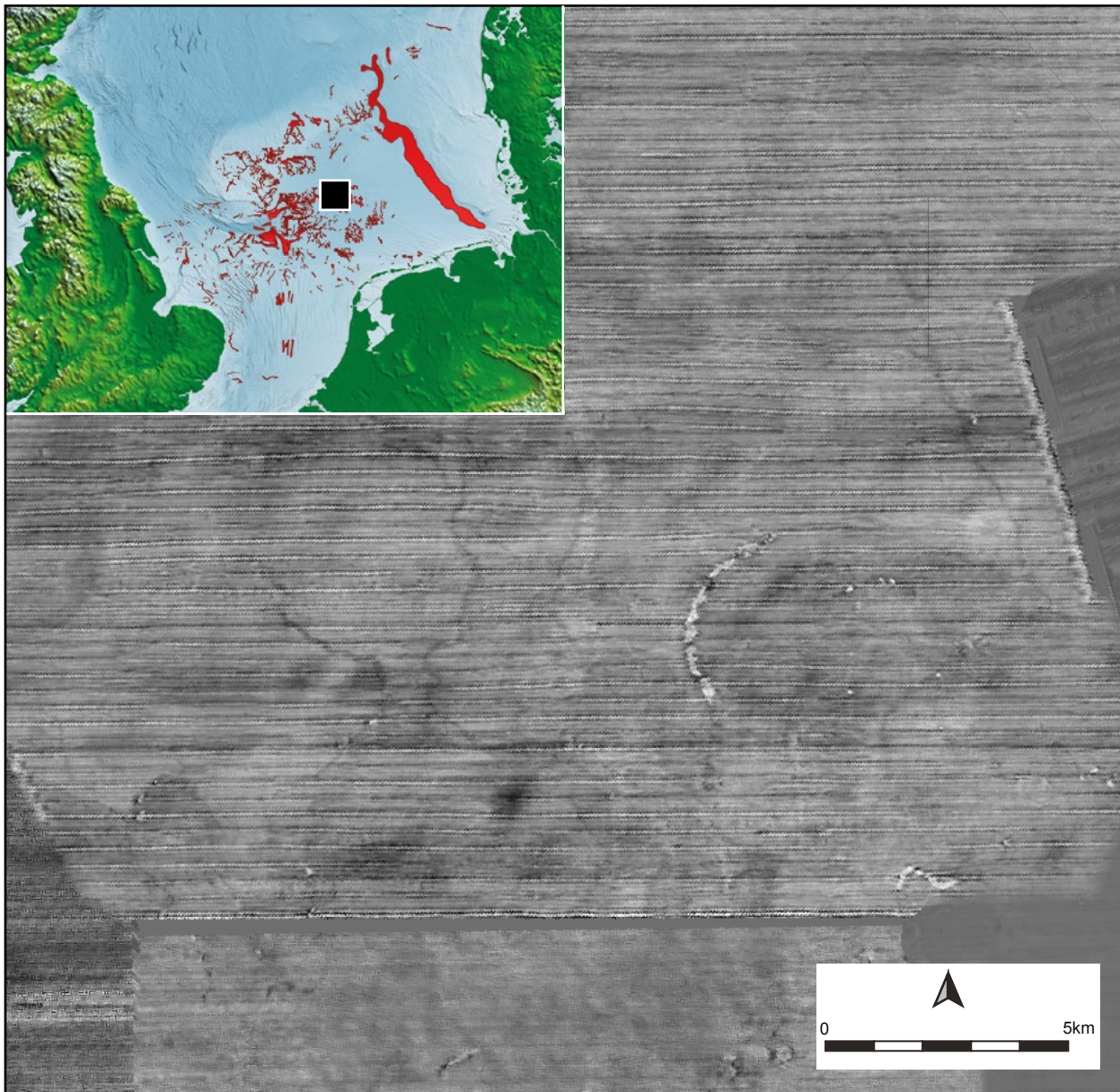


Figure 3.7 Mottling of the seismic data within the Oyster ground can clearly be seen in this image. A number of small palaeochannels can also be seen through the mottling.

palaeovalley, which forms a significant depression in the north-eastern quarter of Area 2 (Figure 3.9, B).

The majority of the fluvial features within the Oyster Ground are oriented to the west, towards the Outer Silver Pit depression and across the large and relatively flat plain (Figure 3.10). The seismic signal generates a ‘mottled’ appearance (Figure 3.10), the origin of which is uncertain but is thought to relate to peat formation in wetlands prior to inundation (Hepp *et al.* 2017). Several small fluvial channels can be observed within this mottled zone (Figure 3.9, C). Although data striping prevents detailed description of these features, they can be seen to flow into a larger channel system which runs along the base of the Dogger Bank. High resolution

2D seismic survey, undertaken as part of the BRITICE project (Roberts *et al.* 2018; 190), crosses this channel and reveals it to be incised up to 20m below the seabed (Figure 3.11). 3D analysis of this channel was undertaken by the authors and TNO staff (Fitch 2011; Van Heteren *et al.* 2014). These revealed phases of development, which are broadly similar to the sequence outlined by Emery (2020: 113 and 165). Proglacial channels are formed, then abandoned and eventually evolve dendritic tributaries as meltwater is replaced by precipitation. They are then transgressed as sea levels rise during the Holocene.

Analysis further reveals the presence of a large channel valley containing evidence for reuse by a small channel

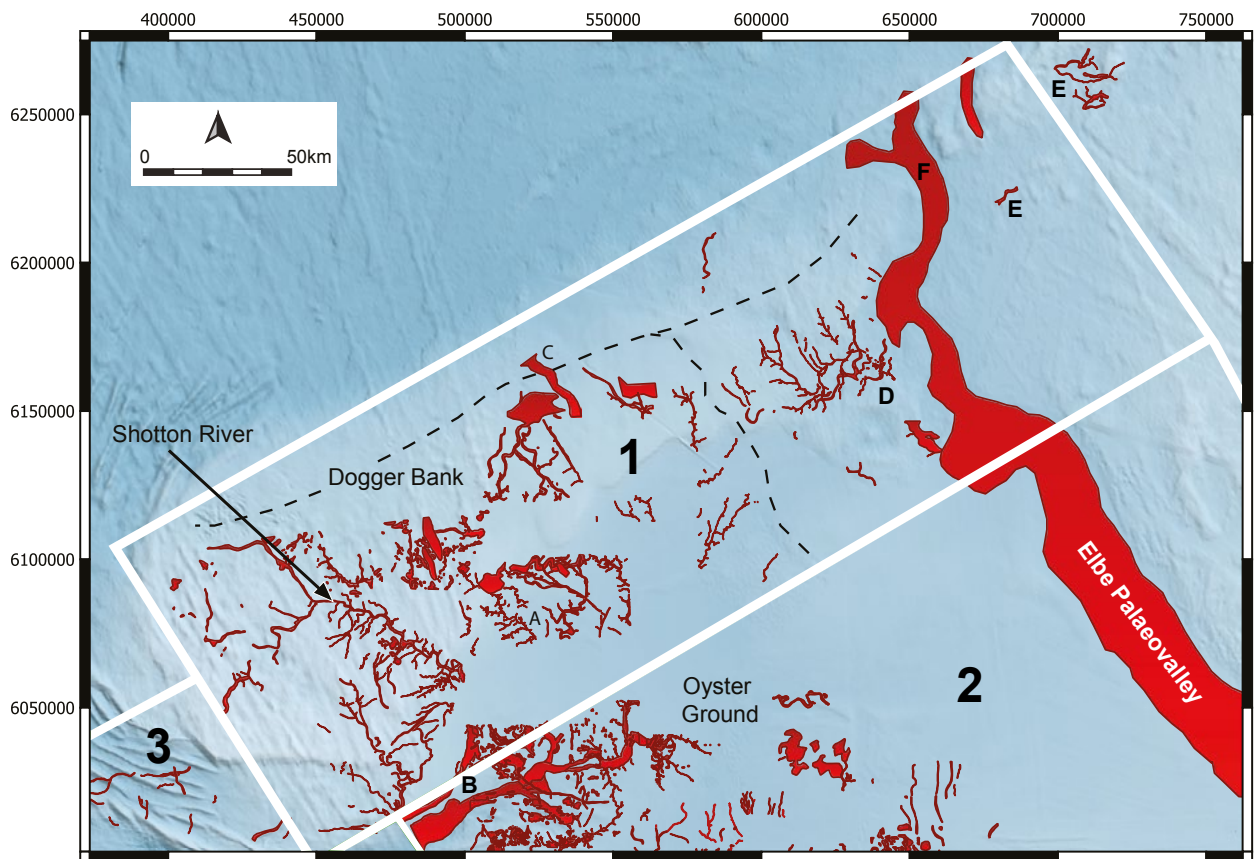


Figure 3.8 Area 1, early Holocene features of the Dogger Bank. The main watersheds are shown as dashed black lines, the features in the southwest of Area 1, including the Shotton River, would have been the longest-lived structures on the Dogger Bank.

(Fitch this volume: Figure 3.5 and 3.9, E). This may suggest such features are the product of proglacial drainage at *c.* 23,000 BP, after the retreat of the ice sheets, and then modified and reused by fluvial channels between *c.* 17,000 to 9000 BP. Later modification is indicated by the formation of tributaries and peat deposits associated with the channels. Dates acquired from nearby cores taken by the BRITICE project (e.g. 175VC Roberts *et al.* 2018) provided early Holocene dates (*c.* 9900 to 9700 BP) but also reveal underlying peat deposits of late Pleistocene age (SUERC-72885, 20,190 \pm 229 cal BP). Fortuitously, one BRITICE core, 147VC, sampled a peat from the Oyster Ground (Figure 3.10), near a likely tributary channel mapped by *Europe's Lost Frontiers*. This provided a C14 date of 12,629 \pm 90 cal BP (SUERC-72883) which clearly indicates the period during which this landscape feature was emergent.

Towards the east of the Oyster ground, a slight topographic high forms a watershed (Figure 3.9, D and Figure 3.12). Holocene palaeochannels flowing east of this rise can be seen in the *Europe's Lost Frontiers* data. These have been independently verified by surveys undertaken in the German sector (Hepp *et al.* 2019) and the Danish Sector (Prins *et al.* 2019). As the *Europe's Lost Frontiers* data extends beyond these datasets, these

channels can be confirmed as flowing into the Elbe palaeovalley. The Elbe remains a significant feature in Area 2 and is represented by a major depression in the bathymetry extending up to the modern coastline and the modern river Elbe.

Small palaeochannels can be observed flowing into the Elbe on both the eastern and western sides of the valley (Hepp *et al.* 2019) and form a significant drainage system within the Doggerland landscape. A study by Papenmeier and Hass (2020), nearer the modern shore, shows this valley to be partially filled with 16m of sediments. In this section of the channel flooding started around 9600 BP and continued to be tidally dominated until *c.* 5000 BP (Papenmeier and Hass 2020).

The Elbe palaeovalley represents an additional *c.* 400km of river length which, combined with the modern Elbe would give the late Pleistocene/early Holocene river a total length of *c.* 1500km. This is, in comparison, greater than the modern length of the Rhine. The size of the valley also reflects the large volumes of water flowing through the extensive drainage system. The channel would have possessed an extremely large catchment, draining parts of Germany, Poland and the Czech Republic. If the submerged section is included, then

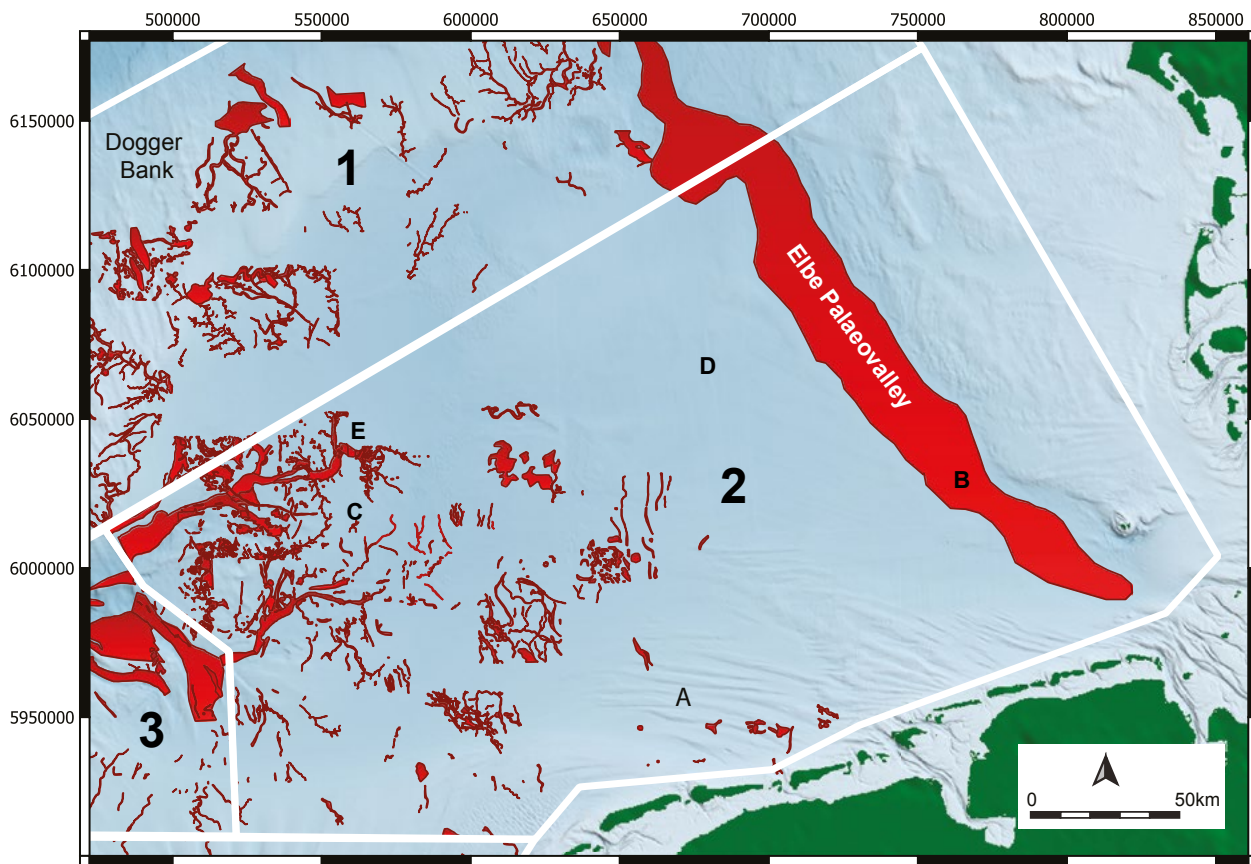


Figure 3.9 Map of the Eastern Sector/Area 2.

this drainage contains parts of Denmark, Netherlands and the Dogger Hills.

Previous researchers have proposed the existence of a palaeolake in the area of the Oyster Ground, formed following glacial melt at approximately 18,700 BP (e.g. Emery 2020; Hijma *et al* 2012; Hjelstuen 2017). This idea originates with Hjelstuen (2017) who suggested that the 12m deep and 3km wide incision at the northeast of the Dogger Bank formed the outflow of such a feature. Hjelstuen's study, however, had no access to seismic data from the area of the hypothesised lake or the Oyster Ground more generally. The suggestion relies on core data from the Ling Bank, which is many kilometres to the north, and well away from the Oyster Ground. Whilst Hjelstuen does acknowledge that there were significant issues in such an interpretation, his work remains the basis for later references to such a feature (e.g., Emery 2020: 119 Fig 4.11).

The 3D and 2D seismic data examined through *Europe's Lost Frontiers*, along with published core data, provides an opportunity to resolve the Oyster ground lake issue. Whilst the data will be discussed in detail in a forthcoming *Europe's Lost Frontiers* volume, no lake deposits were visible within the available seismic data

in this area. It is also clear that there are considerable drainage systems present in the Oyster Ground that would have been able to provide drainage, and these trend to the west and into the Outer Silver Pit. The presence and direction of these channels strongly suggest that the hypothesis that a lake formed in this area, at least, is incorrect. Given that the Outer Silver Pit drains in a different direction, west as opposed to northern outflow proposed by Hjelstuen, it is therefore unlikely that the Oyster ground channels, nor the Outer Silver Pit outflow, is likely to be the source of the delta sediments at Ling Bank identified by Hjelstuen (2017). Indeed, given the presence of a ribbon lake between the ice and the northern edge of Dogger Bank at c. 23,000 to 21,000 BP (Roberts *et al.* 2018), it is possible that this may be the source of the Ling Bank delta material, rather than the Oyster ground. Indeed, Hjelstuen (2017: 16) notes that seismic correlation with sediments from the Ling Bank Delta and shallow bore holes (Hjelstuen 2017: 16) suggests that it was related to the Last Glacial Maximum and therefore could be related to the drainage of the lake observed by Roberts *et al.* (2018: 203) at c. 21,000 BP. It is important to note however that Hjelstuen provides no absolute dating for the Ling Bank sediments and thus the possibility of any correlation remains tentative.

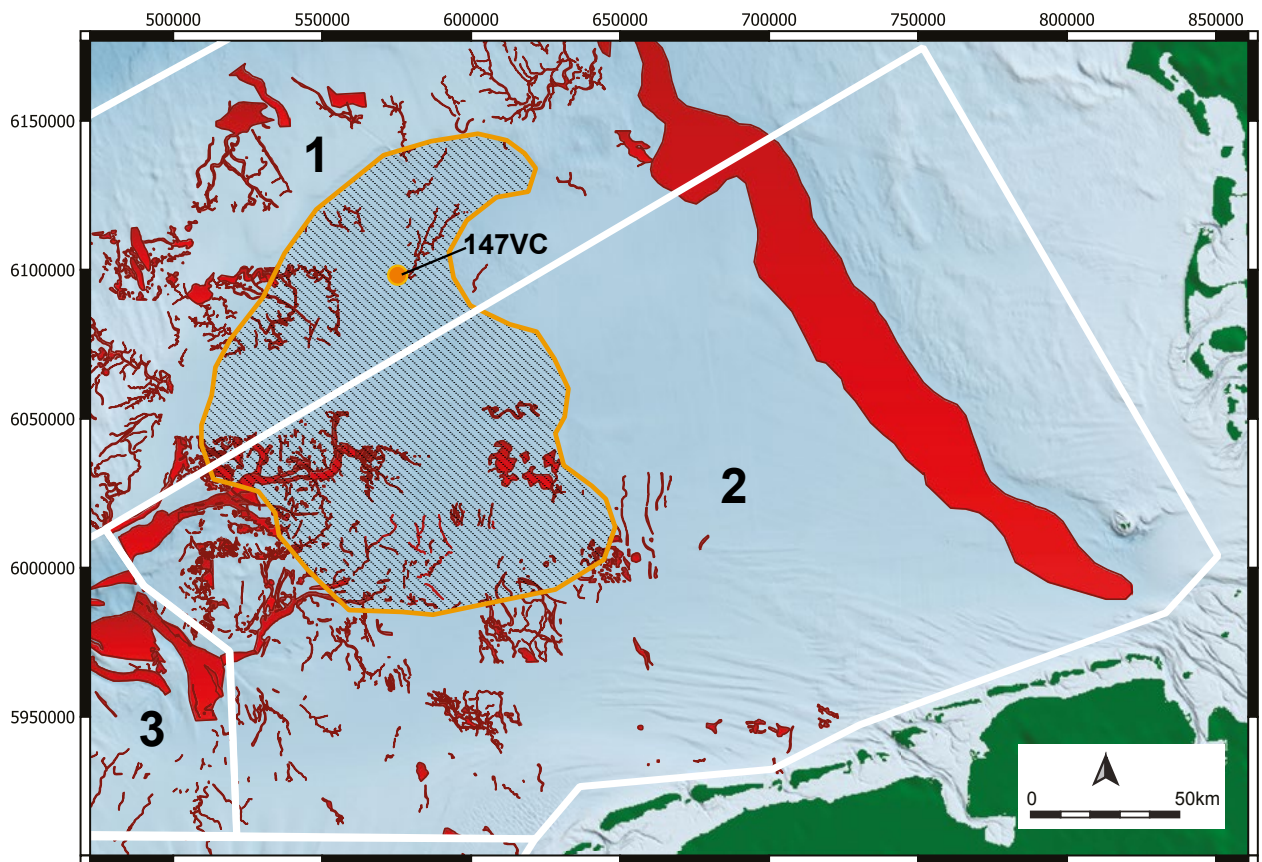


Figure 3.10 The extent of wetland response is outlined within the red hashed area. The location of BRITICE core 147VC is marked in orange.

Other explanations are available for these data. A bathymetric depression (near the area marked 'F' on Figure 3.8) is identified by Hjelstuen as the location of the outflowing of a meltwater burst. However, it must be recognised that this channel cut is the substantial channel associated with the Elbe palaeovalley. There may, therefore, be no need to invoke a lake outburst to explain this depression, indeed, the seismic line presented in the paper (Hjelstuen 2017: Figure 11a) shows the channel to be 15m deep and 3000m wide (Hjelstuen 2017: 14) which is consistent with nearer shore submerged sections of Elbe itself (Papenmeier and Hass 2020), which would not have been affected by a meltwater outburst. It should also be noted that these dimensions are also consistent with other major fluviially derived features within the projects study area that have been recorded by *Europe's Lost Frontiers*.

Finally, it is also important to note that the link to an oxygen isotope anomaly in foraminifera on the Norwegian continental margin, which is dated to c. 18,700 cal BP, and was used by Hjelstuen (2017) to infer the presence of a lake, only indicates the possibility of a meltwater plume near the Norwegian continental margin (Lekens *et al.* 2005). This information does not provide evidence of direction and is not sufficient to tie any possible plume to the Oyster ground area. Indeed,

this plume has previously been identified as coming from the Norwegian Ice Sheet (Lekens *et al.* 2005). Consequently, there is little need to invoke a glacial meltwater palaeolake in the Oyster ground region.

Although the data on the Ling Bank sediments would benefit from further, detailed consideration and dating, the presence of the channel systems in the Oyster ground observed by *Europe's Lost Frontiers* suggest that any palaeolake in the Oyster Grounds is substantially smaller and shallower than suggested, and thus not visible in the data available, or more probably is absent.

Area 3: Western Sector

This area is largely characterised as a relatively gentle plain sloping to the north and down from the modern British coastline (Figure 3.13). The dominant topographic feature within this area is the Outer Silver Pit, which forms a significant depression in the northwest of the area. The Outer Silver Pit is a distinct east-west trending bathymetric deep and is the largest of a series of depressions in the southern North Sea. This feature is up to 80m deep in places and is thought to result either from quaternary sub glacial processes (Praeg 2003), or a catastrophic drainage event

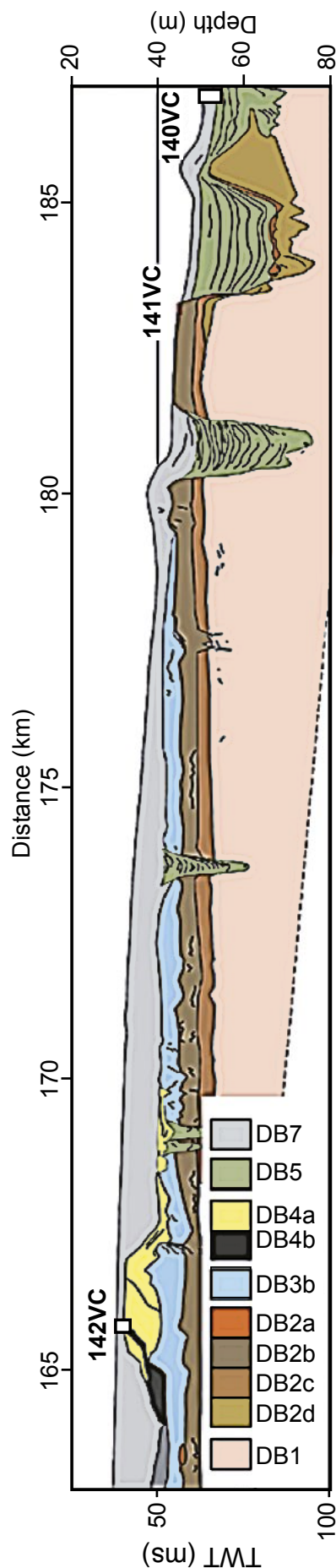


Figure 3.11 Interpretation of a seismic line crossing the base of the Dogger Bank area (near the area marked B in Figure 3.8) clearly shows a large channel running at the base of Dogger Bank (shown here as the DB5 unit between 141VC and 140VC) (Roberts *et al.* 2018; Figure 6).

(Wingfield 1990). This Outer Silver Pit dominates the landscape, with channels from the Oyster Ground (Area 2) flowing into this feature.

The Outer Silver Pit was investigated by the NSPP and thought to have been modified during the Late Palaeolithic/Early Mesolithic by macro tidal processes during marine inundation (Briggs *et al.* 2007: Figure 3.13, A). The Outer Silver Pit was eventually flooded by the sea around 10,000 BP (Shennan *et al.* 2000; Sturt *et al.* 2013). A distinctive zone, characterised by a palimpsest of small channels which cross an area of 5823km², can be seen adjacent to the Outer Silver Pit (Figure 3.13, B). In addition, the area contains several small depressions within which the seismic data is 'mottled'. This mottled signal is thought to indicate peatland/wetland and, consequently, the area, along with the small channels, is thought to represent an extensive wetland area close to the edge of the Outer Silver Pit, which formed an estuary during this period (Briggs *et al.* 2007; Gaffney *et al.* 2007). It is assumed that this wetland environment was continuously active from the end of the Pleistocene until the early Holocene. Recent cores from the area, taken by the BRITICE project (Roberts *et al.* 2018), have recovered peat which dates to 9801 +/- 171 cal BP (SUERC-72162) supporting this hypothesis.

In the centre of Area 3 (Figure 3.13, C), are a series of large anastomosing channels flowing from the southeast and into the Outer Silver Pit. Several of the larger channel features have been associated with the Botney Cut formation and dated to the late Pleistocene to early Holocene (Cameron *et al.* 1992). Detailed survey during the Humber REC over one of the smaller features has revealed that these were active during the Holocene (Fitch this volume; Tappin *et al.* 2011) although coring failed to reach the base of the feature.

A significant outflow channel is partially visible in the southeast corner of the Outer Silver Pit (Figure 3.13, D). This appears to drain the Outer Silver Pit to the south and is of a sufficient size for the channel to have a contemporary bathymetric expression. Imaging this feature using 3D seismic data suggests that the channel must have been formed following a considerable outflow, and that it extends much further south than is visible on the bathymetry. Although no dating evidence from this feature is currently available, the presence of a small number of re-use channels suggests that the feature is of pre-Holocene age. The current models for the last glaciation suggest two possible points of origin for this feature (Roberts *et al.* 2018). The first requires an outflow from the lake in the Outer Silverpit (referred to as 'Dogger Lake' by Roberts *et al.* 2018: Fig 17), and which may have occurred a short time prior to 30,000 BP. Roberts *et al.* (2018) note that sometime between 30,000 to 25,000 BP, following an ice advance, a separate glacial lake was moved eastwards by the ice from the

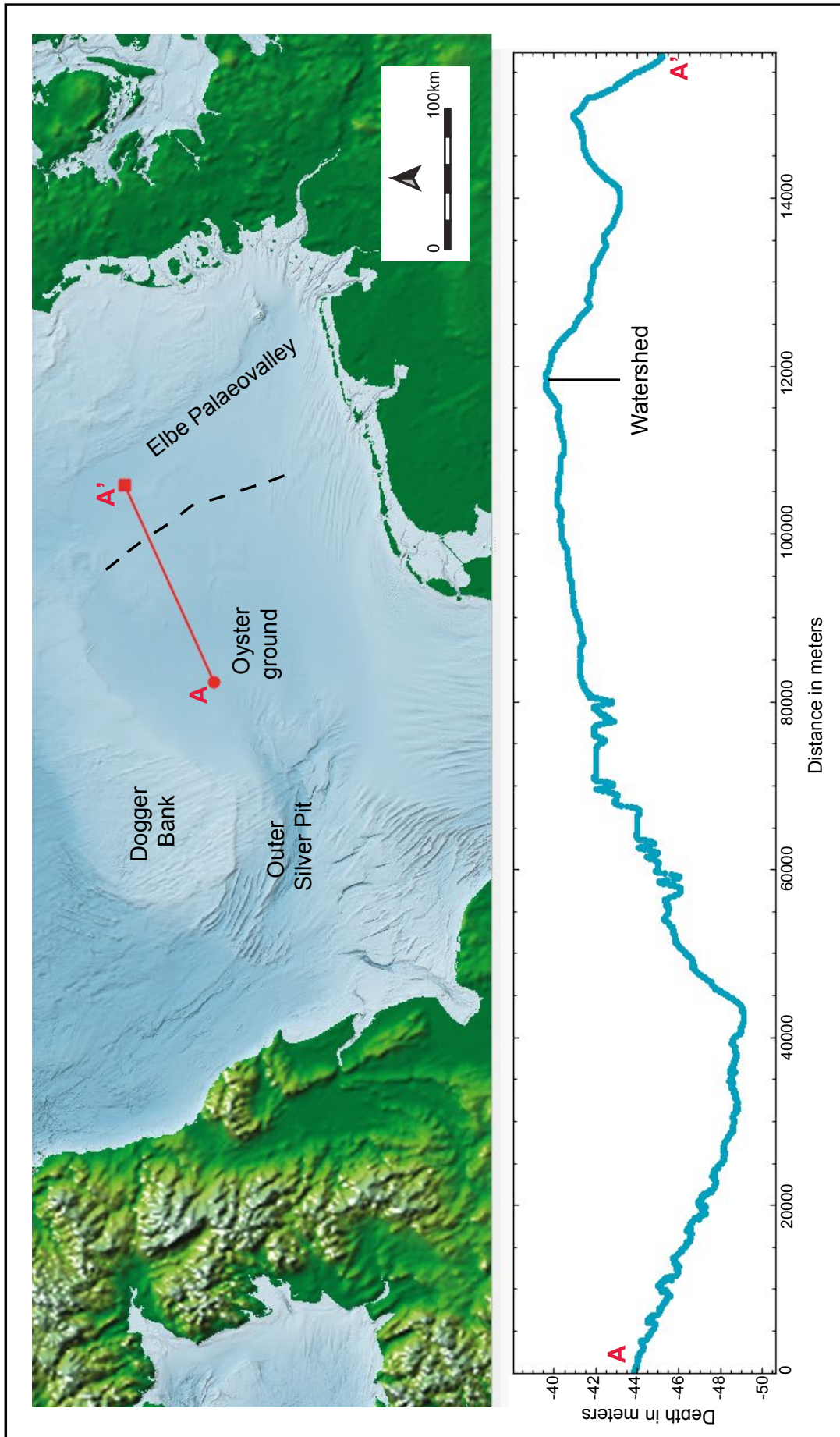


Figure 3.12 Cross section across the east of the Oyster ground. The topographic rise which forms the watershed is apparent.

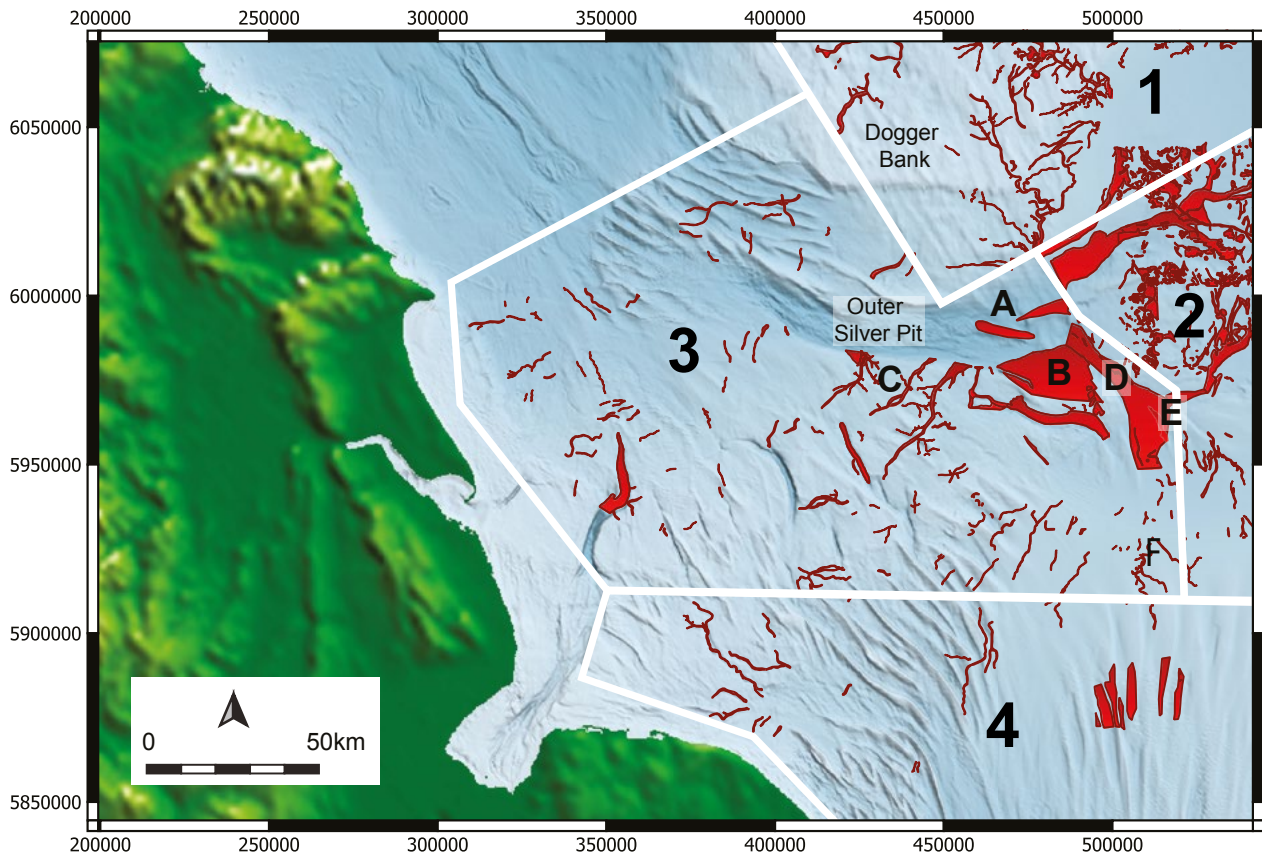


Figure 3.13 Location of mapped features within Area 3.

area around the Outer Silver Pit to the northeast of the Dogger Bank. This water movement may have provided the opportunity to breach the Outer Silver Pit banks to the south and produce a meltwater outburst that could have, feasibly, created this feature. The second point arises during the 22,000 to 21,000 BP ice advance. Around 23,000 BP, a ribbon lake had formed to the north of the Dogger Bank (Roberts *et al.* 2018), and it is possible that this feature may have extended around the Dogger Bank into the Outer Silver Pit. Ice re-advance beginning at c. 22,000 BP may then have pushed into the area of the ribbon lake and induced an outburst from the lake creating this feature. Whilst it is impossible currently to provide an accurate date for origin of the channel, its size, position, and the evidence for later re-use suggest that it was a significant feature within the Holocene landscape, and that it was a route for flooding from the south during final inundation.

Slightly to the east of the outburst channel, close to the boarder with Area 2, is another large, deeply incised channel system (Figure 3.13, E). This is c. 1400m wide and appears to drain part of the Oyster Ground (Area 2). It can be seen to flow southwest in the seismic data, before eventually meeting the large outflow channel south from the Outer Silver Pit. At this point the channel changes direction, re-uses the outflow channel, and

flows south. This relationship suggests that the channel (Figure 3.13, E) is later than the outwash feature (Figure 3.13, D), and dates from a period either post c. 30,000 BP or c. 21,000 BP.

The presence of this channel is also indicated in a map of the area by Emery (2020: 119 Figure 4.11), and the feature may drain some of the European rivers prior to the formation of the Elbe palaeovalley). However, Emery emphasises the speculative nature of this interpretation, and the seismic data is unable to provide sufficient evidence of any extension to the Elbe Palaeovalley channel to support this suggestion. As the channel links with dendritic feeders where it extends into Area 2, this suggests that the feature was sub-aerially exposed during the Holocene and thus remained a feature in the landscape throughout the late Pleistocene/Holocene period.

The southwards trend of this large feature is paralleled by several smaller channels (Figure 3.13, F), one of which was recorded by Preag who suggested a Holocene date for the feature (1997). The *Europe's Lost Frontiers* 3D seismic interpretation suggests that this channel, and those nearby, have a well-developed, high sinuosity. The *Europe's Lost Frontiers* data also reveals additional features related to these features, including floodplains, bars and oxbow

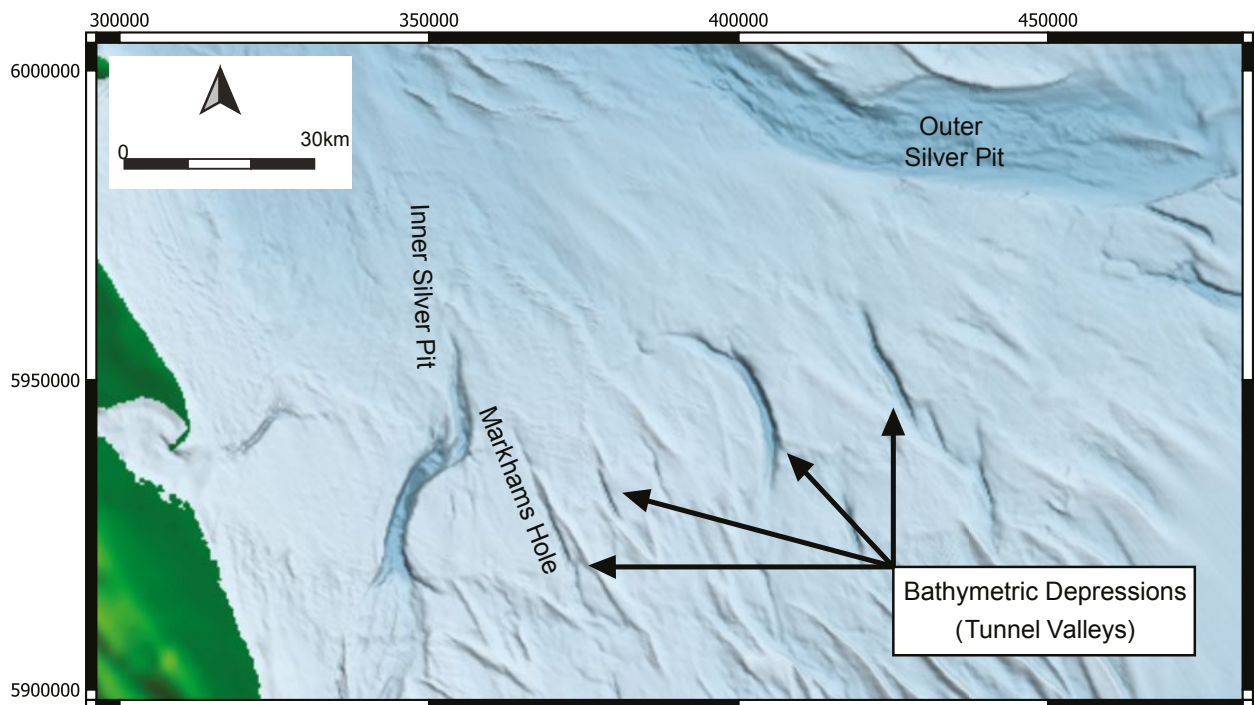


Figure 3.14 Topographic depressions southeast of the Outer Silver Pit (Area 3)

lakes, which illustrate the development of this plain. Many of the channel features recorded are comparable to those seen in the Danish sector (Prins and Andersen 2019), and presumably form at a similar time and environment. It is apparent that several of the features are well preserved and within reach of future high resolution geophysical survey and environmental sampling.

The western part of this landscape includes a number of large depressions, including Markham's Hole (Figure 3.14), which are tunnel valleys and may have contained lacustrine features during the Mesolithic. The seismic data reveal that these features are much deeper than the bathymetry suggests and contain deposits that can be directly related to the late Pleistocene, Botney Cut Formation. The late Pleistocene sediments are then directly overlain by sediments of recent origin. The sedimentary relationships therefore suggest that the valleys date from the late Pleistocene. As these features would have formed topographic features in the Holocene landscape, it is likely that these depressions may have contained lakes during the Early Holocene. This interpretation is supported by the work of the British Geological Survey (Brown 1986), who records the presence of late Weichselian to Holocene glacio-lacustrine deposits in similar features in the British sector.

Area 4: Southern Sector

Although it is suspected that Area 4 (Figure 3.16) has significant information relating to the early Mesolithic landscape, data striping and noise in the 3D seismic

data hindered interpretation. Fortunately, new 2D seismic data acquired during windfarm development, and research surveys undertaken as a collaboration between *Europe's Lost Frontiers* and the Deep History Project, provides valuable supplementary information for the area (e.g., Messiaen *et al* 2020). The expansion of windfarms within this area will also offer future opportunities to significantly refine and improve the mapping for this area (Peeters *et al* 2019).

A brief description of the area and the results of survey are provided here, more detail will be provided in a later volume (Fitch *et al*. forthcoming). Whilst the details of the majority of the channels observed are yet to be fully resolved, they do tend to be smaller in scale than those discussed in the other mapping areas of the study area.

The lack of palaeochannels within this area is striking (Figure 3.15). The central zone within Area 4 is totally devoid of these features (Figure 3.15, A). Those that do exist (e.g. the Southern River, Figure 3.15, B) are scattered toward the periphery of the area, but appear to flow towards the central axial area between East Anglia and the Netherlands (Figure 3.16) and seem to terminate at or near the 40m meter bathymetric contour. This dearth of landscape features in the central zone is probably explained by the presence of a large marine embayment infilling during the Mesolithic. Isostatic models (e.g. Sturt *et al*. 2013), and more recent models utilising improved core data from the region (Ch'ng *et al*. forthcoming), suggest that flooding of this area was initiated by 10,500 BP. This is supported

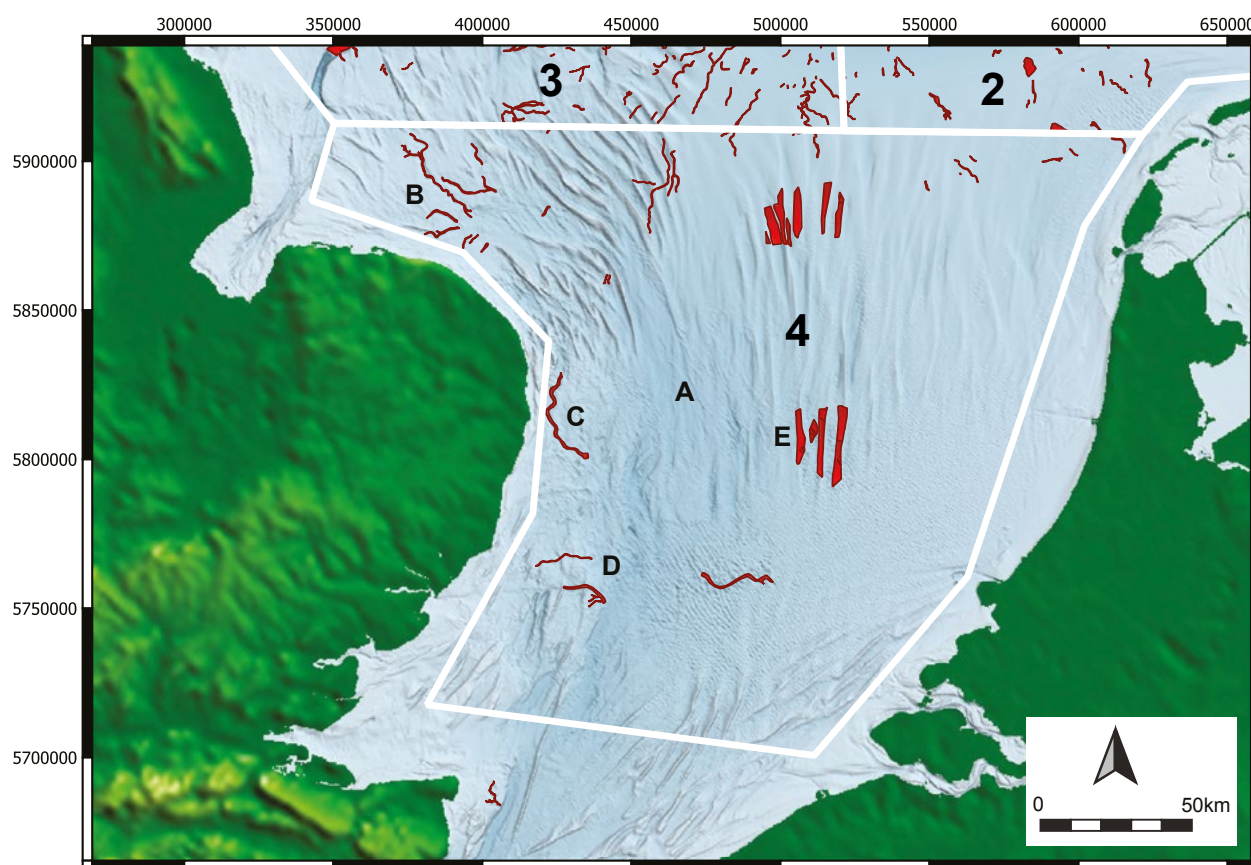


Figure 3.15 Early Holocene landscape features in Area 4.

by core data from the Belgian continental shelf which indicates marine influence in the area at 10,000 BP and possibly earlier (De Clercq 2018). A core (VC39), taken by the TNO in 2019 near the Brown Bank, also provides a sea-level index point at 10,280 \pm 77.5 cal BP (Busschers pers. comm.). This information, combined with radiocarbon dates from the estuary of Southern River (VC51: 8827 \pm 30 cal BP, SUERC-85716), strongly support the existence of a marine inlet in this area during the Mesolithic.

Of the palaeochannels that are visible, the majority are situated on the western flank on the East Anglian shelf (Figure 3.15, C and D). These channels are characterised by broad, but shallow, meanders, suggestive of a gentle water flow. The channels can be seen to widen as they progress towards the marine inlet, indicating the direction of flow. Mapping of these features suggest that the heads of the channels are filled with fine grained sediment and organic material (possibly peats) as the channels approach the contemporary coastline, the seismic signal suggests this material then progresses into silts and clays. This sequence of sediments is similar to those seen in other channels in the southern North Sea (e.g., Missiaen *et al.* 2020, Fitch *et al.* this volume) and a description is provided by the East Coast Regional Environmental Characterisation

(ECREC, Limpenny *et al.* 2011). A single vibrocore acquired from one channel (Figure 3.15, C) recovered peats dated at 10,670-10,250 cal BC (SUERC 11978) at 30.80m deep and 7530-7350 cal BC (SUERC 11975) at 30.05m deep (Limpenny *et al.* 2011: 131). These dates are broadly comparable to those from near the Brown Bank on the eastern bank of the embayment (8,716-8,566 cal BC (SUERC 89491)), and Southern River (ELF051 (2.84m): 7844-7606 cal BC (SUERC 85724), ELF051 (3.78m): 11,080-10,854 cal BC (SUERC 85725)). The termination of these palaeochannels at or near the c. 40m meter bathymetric contour, suggests a period of coastal stability. However, it may also be true that subsequent flooding did not result in erosive conditions comparable to those during the initial formation of the central marine inlet, possibly because the widening channel may have induced lower current speeds.

Fewer channels are observed within the available 3D seismic data on the eastern flank of the marine inlet. However, high resolution survey, undertaken as part of the Deep Sea History collective, combined with data from recent windfarm projects, has demonstrated that there are Holocene deposits in the region, and those channels which have been cored are sand filled, and often have organic rich and occasionally peat layers (Harding *et al.* forthcoming, Missiaen *et al.* 2020, Plets *et*

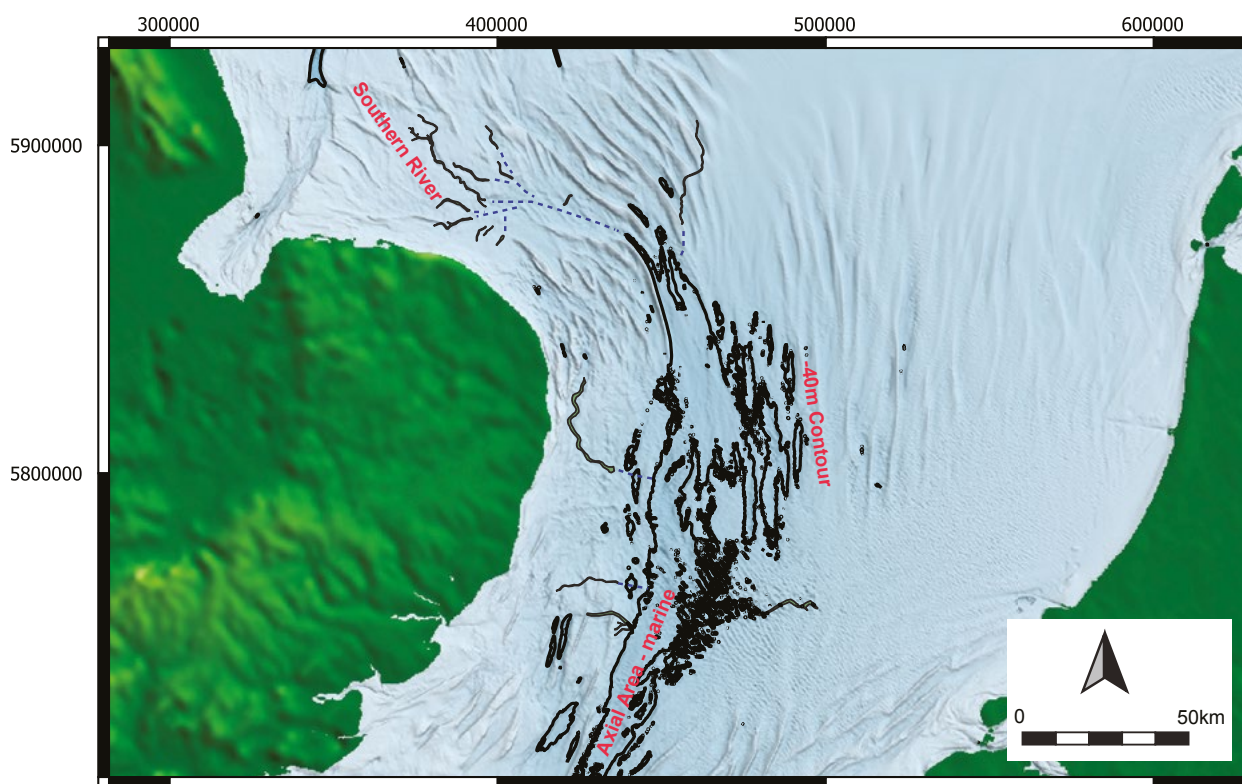


Figure 3.16 Mapped palaeochannels in Area 2 flow towards the -40m bathymetric contour, below this line virtually no features are mapped. This supports the hypothesis that the axial area was a marine inlet during the Holocene/Mesolithic.

al. forthcoming, Thal 2019). Aside from palaeochannels, land surfaces are occasionally visible (*Harding et al. forthcoming: Figure 3.15, E*), which are overlain by organic layers, intertidal deposits and frequently buried under sandbanks. These surveys have also provided a clear, acoustically strong high amplitude signal in the seismic data which has been identified as the top of the Naaldwijk Formation and associated with the marine inundation of the area. Landsurfaces associated with the Naaldwijk Formation may provide responses characterised by a coherent negative, flat parallel reflection. These are often regarded as indicative of peat layers (e.g. *Plets et al. 2007*). These peats are thought to have formed as the post-glacial soils were impacted by higher levels of salinity, sedimentary accretion and flooding (*Andrews et al. 2000*). The base of the Naaldwijk Formation is poorly resolved further east, possibly due to a lack of signal penetration resulting from the increasing thickness of the overlying sand banks.

Any palaeochannels that may have existed in the central zone in the Late Palaeolithic (pre-10,000 BP) were presumably impacted by marine erosion following formation of a marine inlet. As the area of the inlet was inundated and exposed to marine erosion at a relatively early date, the chances of such features surviving is presumably significantly lower.

Area 2 also possesses significant surface topography and modern (less than 4000 BP) seafloor features including sand waves. These structures are imaged in the bathymetry as north-south-trending peaks and troughs. The modern sediments have an erosional contact with the Holocene. Several modern sandbanks also directly overlie and preserve areas of Holocene landscape (e.g. the Brown Bank *Missiaen et al 2020: Figure 3.15, E*). Consequently, the modern bathymetry does not necessarily reflect the Holocene landscape morphology in this area. Additionally, the size of many of these sandbanks can render the underlying Holocene landscape relatively inaccessible to archaeological sampling. However, where topographic or erosional conditions allow, it is possible to recover sediment samples, as has been successfully demonstrated near Brown Bank (*Missiaen et al 2020*).

An archaeological narrative of landscape development from the Late Palaeolithic to the Mesolithic

Having provided a general description of landscape features identified during recent study, it is useful to support this with a summary chronological and archaeological overview.

At the end of the Late Palaeolithic, the northern edge of the current Dogger Bank essentially represented

the coastline of Doggerland (Figure 3.17). Although the Outer Silver Pit and the embayment to the south, near Brown Bank, had already started to flood, research by BRITICE suggests that the coastline north of Dogger Bank had existed from c. 21,000 BP (Roberts *et al.* 2018). This coastline remained a relatively stable component of the landscape for approximately 11,000 years prior to the start of the Mesolithic. The implications of a relatively stable northern coastline are significant. The coastline, with its rich and varied resources must have been extremely important in economic and cultural terms to the human communities in the region.

As sea levels rose there would have been impacts affecting large areas away from this coastline. The Outer Silver Pit would have become a significant marine inlet, and an outlet for major drainage systems from the Dogger Bank and East Anglia (Figure 3.17). The other main drainage basin, associated with the Elbe palaeovalley, would have experienced flooding with a significant inlet forming on the north-eastern coastline of Doggerland. Whilst these areas flooded, the Elbe palaeovalley channel would have continued to drain areas in the east of Doggerland, as well as Denmark and Germany (Figure 3.17). Inundation would also have continued in the south of Doggerland. Here, flooding would have preceded from the area of the English Channel (Figure 3.17) and created a relatively shallow marine inlet between Britain and the Netherlands (Figure 3.18). Although low lying, most of the study area remained emergent during this time and the landscape

could have provided a diversity of environments that would have made the area attractive for a range of subsistence activities. The extensive river systems would have provided excellent transport corridors for both human and animals, as well as providing wetland resources. Given the connectedness of the landscape, it is reasonable to surmise that groups from what are now the Netherlands and Britain were connected through Doggerland (Reyneir 2000 citing Verhart pers. comm.). Aside from connections across the land, the boat technology of the day must have supported travel (Pedersen *et al.* 1997), supporting trade and contact between communities who lived in or visited the region (Gaffney *et al.* 2009). A number of cultural indicators are suggestive of such links. These include the rare antler head dresses, found at Bedburg-Konigshoven in Germany (Street 1989), through the Low Countries (Verhart 2008) and as far north as Star Carr (Clark 1972; Conneller 2004). Such linkages may suggest a 'northern technocomplex' centred on the great plains of the North Sea (David 2006: 139).

Between 10,000 BP and 8500 BP sea-level rise continued and large tracts of the landscape of central Doggerland must have been inundated, initially through the three main inlets in the landscape (Figure 3.18). The area around the Outer Silver Pit was submerged, allowing the inundation of large parts of the centre of Doggerland including the relatively low-lying area of the Oyster Ground.

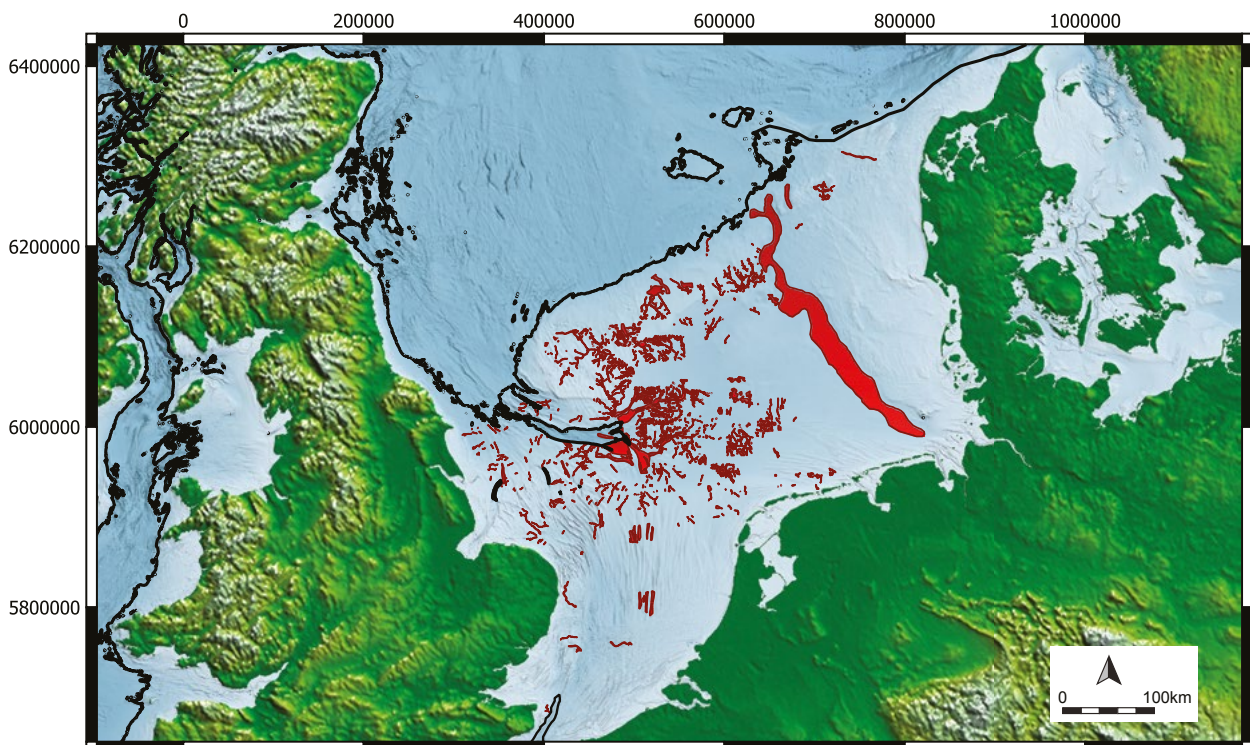


Figure 3.17 Major features, Late Palaeolithic c. 11,500 BP.

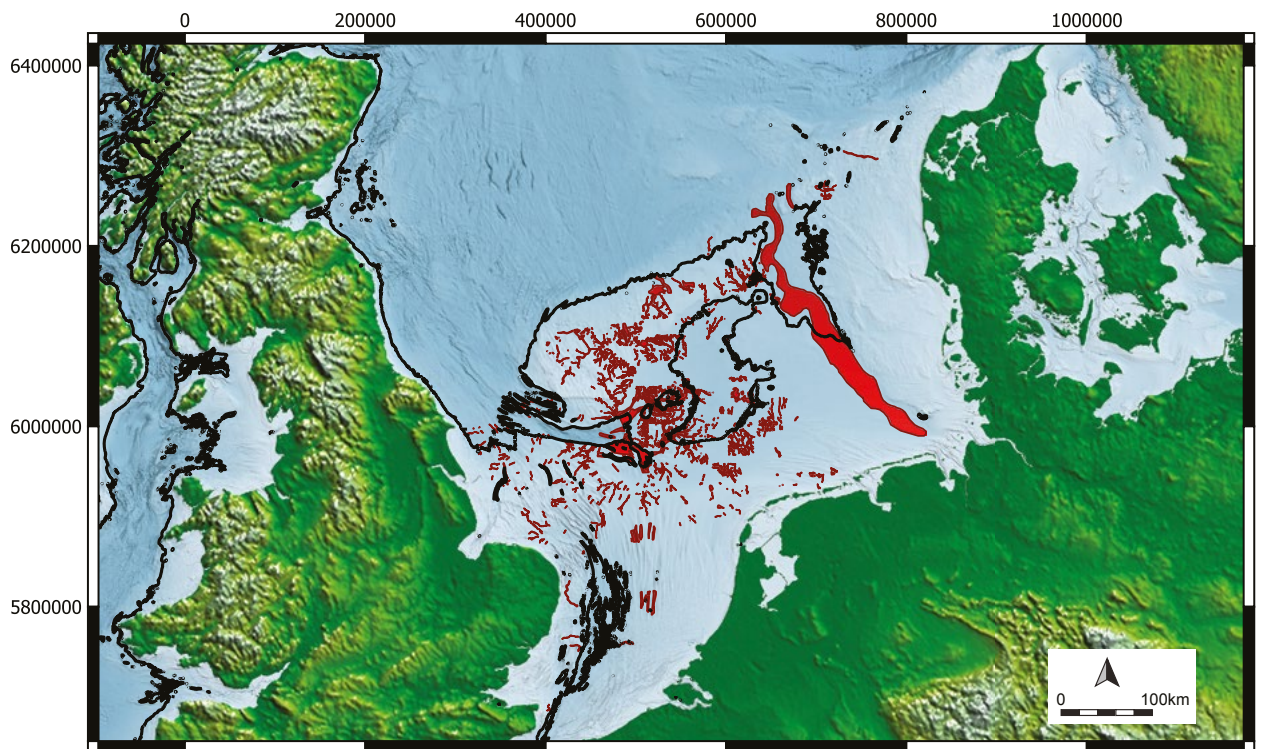


Figure 3.18 Coastlines of early Mesolithic Doggerland c. 10,000 BP.

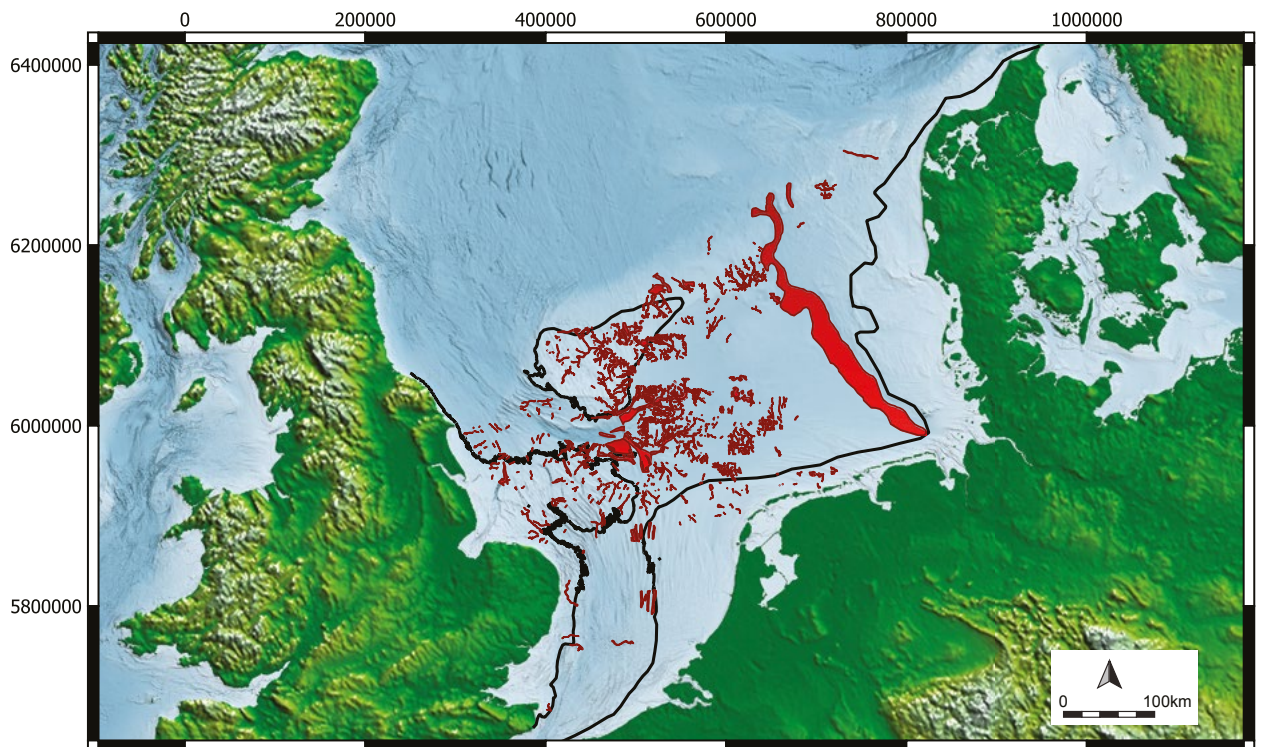


Figure 3.19 Coastlines of Mesolithic Doggerland c. 8500 BP.

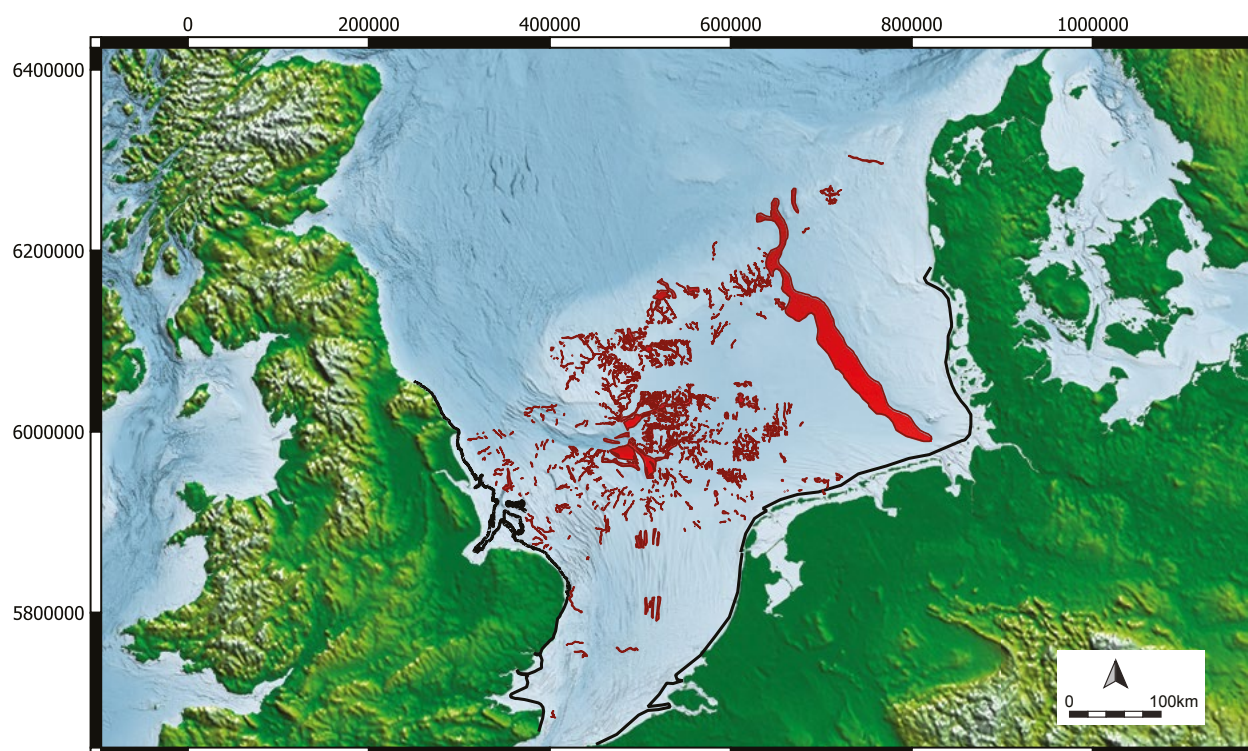


Figure 3.20 Coastlines of the earliest Neolithic c. 7000 BP.

It is during this period that the Dogger Bank became an island (Figure 3.19). Its links to the east were cut as waters flooded the Elbe palaeovalley. Additionally, with the coastline retreating from the south and into the central part of Doggerland, the terrestrial linkage between Britain and Europe would have rapidly reduced to a strip and was eventually breached. These relatively rapid changes presumably had an impact on the Mesolithic communities inhabiting the new coastlines. Not all change was bad. New coastlines may have provided access to marine resources and enhanced the subsistence base for coastal communities, who may have also taken advantage of the new marine inlets for travel.

As the landscape fragmented and terrestrial interconnectivity reduced (Figures 3.18 and 3.19), it is possible that the groups living in this area may have found maintaining traditional links increasingly difficult. It is possible that connections were severed even before the inundation of the final land linkages.

By about 7000 BP, the emergent landscape of Doggerland was largely lost to the sea (Figure 3.20).

During this period, Britain and Europe were separated by a considerable body of water and the Dogger Island would have been flooded. However, areas of landscape would still have existed as extensions of East Anglian and the European coastlines at the end of the Mesolithic and into the Neolithic (Figure 3.20). Continuing sea-level rise and loss of landscape would have remained noticeable to contemporary communities and was likely to have influenced the cultural development of these regions.

Conclusions

Europe's Lost Frontiers and its preceding projects have enabled a significant advance in our understanding of the emergent landscape of the southern North Sea and provided first pass mapping of an area of prehistoric landscape of c. 188,000km². The full archaeological implications of this work will be explored in later project volumes but will also act as a springboard for future researchers studying climate, sea-level history, palaeogeography, geology as well as archaeology.